

Supporting Information

A Wide-bandgap D-A Copolymer Donor Based on Chlorine Substituted Acceptor Unit for High Performance Polymer Solar Cells

Tao Wang^{1,#}, Rui Sun^{1,#}, Shengjie Xu², Jie Guo¹, Wei Wang¹, Jing Guo¹, Xuechen Jiao^{3,*}, Jianbo Wang⁴, Shuangfeng Jia⁴, Xiaozhang Zhu^{2*}, Yongfang Li², Jie Min^{1,5,6*}

1 T. Wang, R. Sun, J. Guo, Prof. J. Min

The Institute for Advanced Studies, Wuhan University, Wuhan 430072, China

2 S. Xu, Prof. X. Zhu, Prof. Y. Li

Beijing National Laboratory for Molecular Sciences, CAS Key Laboratory of Organic Solids, Institute of Chemistry, Chinese Academy of Sciences, Beijing 100190, China

3 Dr. X. Jiao

Department of Materials Science and Engineering, Monash University, Victoria, Australia; Australian Synchrotron, Clayton, VIC, Australia

4 S. Jia, Prof. J. Wang

School of Physics and Technology, Center for Electron Microscopy and MOE Key Laboratory of Artificial Micro- and Nano-Structures, Wuhan University, Wuhan 430072, China

5 Prof. J. Min

Key Laboratory of Materials Processing and Mold (Zhengzhou University), Ministry of Education, Zhengzhou, 450002 China

6 Prof. J. Min

Key Laboratory of Organofluorine Chemistry, Shanghai Institute of Organic Chemistry, Chinese Academy of Sciences

*E-mail: min.jie@whu.edu.cn; xzzhu@iccas.ac.cn; xuechen.jiao@monash.edu

[#]The first two authors contributed equally to this paper.

Experiment Section

Materials and synthesis

Compound M1 was synthesized according to the previously reported methods with high yield.^[1] Synthesis started from 4,5-dichlorobenzene-1,2-diamine (1), which was reacted with sodium nitrite to yield compound 2, and compound 2 was chosen as the π -electron-deficient component. Then, the alkylation of compound 2 was produced by reacting 1-bromo-2-hexyldecane with anhydrous potassium carbonate in *N,N*-dimethylformamide at 150 °C for 12 hours. Compound 3 was first activated by forming an intermediate 4 with a trimethylsilyl group. Subsequently, compound 5 was synthesized by bromination with liquid bromine and chloroform at 60 °C for 24 hours, shielded from light. After this, compound 5 was reacted with 2-(tributylstannyl)thiophene via a Stille coupling reaction to produce compound 6. The monomer M1 was obtained by brominating the compound 6 with *N*-bromosuccinimide (NBS). Finally, the target polymer J101 was synthesized by a typical Stille polymerization using anhydrous toluene as solvent and tetrakis(triphenylphosphine)palladium (0) [Pd(PPh₃)₄] as a catalyst at 110 °C for 17 hours. The polymer J101 was carefully purified by continuous Soxhlet extractions with methanol, hexane, acetone, and chloroform, then chloroform fraction was concentrated under vacuum evaporation, precipitated into methanol. Finally, the crude product was collected by filtration and dried under vacuum at 40 °C for 16 hours. The polymerization yield of 53.7% was obtained. J101 has good solubility in common organic solvents such as chloroform, chlorobenzene, and o-dichlorobenzene.

Compound M2 and J71, ITIC were purchased from Solarmer Materials Inc. ZITI was provided by Xiaozhang Zhu's group. 4,5-dichlorobenzene-1,2-diamine, sodium nitrite, acetate, anhydrous potassium carbonate, *N,N*-dimethylformamide, 1-bromo-2-hexyldecane, lithium diisopropylamide (LDA), chlorotrimethylsilane, bromine (Br₂), chloroform, 2-(tributylstannyl)thiophene, *N*-bromosuccinimide (NBS), tetrakis(triphenylphosphine)

palladium (0) [Pd(PPh₃)₄], bis(triphenylphosphine)palladium(II) chloride [Pd(PPh₃)₂Cl₂] were purchased from commercial sources and used as received. Tetrahydrofuran (THF) and toluene were distilled under nitrogen protection Na/benzophenone before reaction.

Compound 2-6, M1 and J101 were well characterized by ¹H or ¹³C-NMR.

Compound (2), the commercial 4,5-dichlorobenzene-1,2-diamine (1) (4.54 g, 25 mmol, 1 eq) was dissolved in glacial acetic acid (3 mL) and water (100 mL) and cooled down to 0 °C. A solution of sodium nitrite (1.92 g, 27.5 mmol, 1.1 eq) in water (40 mL) was added dropwise and stirred at this temperature for 2 hours. Then the reaction mixture was allowed to room temperature and stirred for overnight. The crude product was filtered, washed with water and dried in vacuum. The product was used for next-step without further purification.

Compound (3), (2) (4.21 g, 22.5 mmol, 1eq), anhydrous potassium carbonate (3.78 g, 27 mmol, 1.2 eq) were put into a 250 mL two-neck round bottom flask, and then added *N*, *N*-dimethylformamide (100 mL). Subsequently, 1-bromo-2-hexyldecane (7.08 g, 22.5 mmol, 1eq) was added dropwise, and the mixture stirred at 150 °C for 12 hours under argon protection. After cooling down to the room temperature, the mixture was poured into water (300 mL) and then extracted with dichloromethane for several times. The combined organic phase was washed with water for twice and then dried over anhydrous magnesium sulfate. After the solvent was removed by rotary evaporation, the crude product was purified by column chromatography (eluent: dichloromethane: petroleum ether = 1:10, *R*_f = 0.317) on a silica gel to give compound 3 as a colorless oil. (6.21 g, yield: 67%). ¹H-NMR (400 MHz, Chloroform-*d*) δ 8.00 (s, 2H), 4.59 (d, *J* = 7.0 Hz, 2H), 2.22 (m, 1H), 1.29-1.19 (m, 24H), 0.86 (m, 6H).

Compound (4), lithium diisopropylamide (LDA) (14.7 mL, 29.4 mmol, 2 M, 2.2 eq) was added dropwise to a solution of (3) (5.47 g, 13.3 mmol, 1 eq) in anhydrous THF (80 mL) under a nitrogen atmosphere at -78 °C. The reaction mixture was stirred at this temperature for 1 hour. Subsequently, trimethylchlorosilane (3.45 g, 31.12 mmol, 2.34 eq) in anhydrous THF (20 mL) was added dropwise to the reaction solution and stirred at this temperature for 3 hours. After

that, the mixture was poured into saturated ammonium chloride solution and extracted with chloroform. The combined organic phase was washed with water for twice, then dried over anhydrous magnesium sulfate, filtered and concentrated under reduced pressure. The product was directly used for the next reaction without any purification.

Compound (5), (4) (6.22 g, 11.19 mmol, 1eq) and chloroform (60 mL) were added into two-neck round bottom flask. Then liquid bromine (89.52 mmol, 4.60 mL, 8 eq) was added dropwise at room temperature. The solution was then stirred at 60 °C for 24 hours in the dark. After cooling down to the room temperature, the mixture was poured into saturated sodium hydroxide solution (200 mL) and extracted with dichloromethane for several times. The crude product was further purified with silica column chromatography using petroleum ether and dichloromethane (10:1, $R_f = 0.436$) as eluent to get faint yellow oil. (3.12 g, yield: 49%). $^1\text{H-NMR}$ (400 MHz, Chloroform-*d*) δ 4.64 (d, $J = 7.3$ Hz, 2H), 2.35-2.26 (m, 1H), 1.33-1.18 (m, 24H), 0.85 (m, 6H).

Compound (6), 5 (0.81 g, 1.41 mmol, 1eq) and 2-(tributylstannylyl)thiophene (1.20 g, 3.1 mmol, 2.2 eq) were added into anhydrous toluene (50 mL). $\text{PdCl}_2(\text{PPh}_3)_2$ (0.05g, 0.07 mmol, 0.05 eq) was added quickly under nitrogen atmosphere. The reaction mixture was stirred at 110 °C for 48 hours. Then cooled down to room temperature, the reaction mixture was poured into water (200 mL) and extracted with dichloromethane for several times. The organic layer was washed with water for twice, dried over anhydrous sodium sulfate, filtered and concentrated under reduced pressure. The crude product was purified by column chromatography (eluent: dichloromethane: petroleum ether = 1:10, $R_f = 0.323$) on a silica gel to give compound 6 as a yellow oil. (6.21 g, yield: 67%). $^1\text{H-NMR}$ (400 MHz, Chloroform-*d*) δ 8.00 (dd, $J = 3.7, 1.2$ Hz, 2H), 7.62 (dd, $J = 5.2, 1.2$ Hz, 2H), 7.29-7.27 (m, 2H), 4.68 (d, $J = 6.8$ Hz, 2H), 2.34-2.26 (m, 1H), 1.35-1.27 (m, 24H), 0.92 (m, 6H).

Synthesis of (M1). Compound 6 (0.47 g, 0.82 mmol, 1 eq) was dissolved in *N,N*-dimethylformamide (15 mL) in a dried flask. The mixture was cooled to 0 °C in an ice bath. Then, *N*-bromosuccinimide (0.37 g, 2.05 mmol, 2.5 eq) was added in one portion under the

darkness. Then the solution was stirred at 0 °C for 15 minutes, the mixture was stirred at room temperature for 36 hours and then quenched with water (200 mL). The solution was extracted with chloroform and washed with water for three times, sequentially. The solvent was removed under reduced pressure, and the residue was further purified with silica column chromatography using dichloromethane and petroleum ether (1:10, R_f = 0.58) as eluent to afford the compound M1 as bright yellow solid (0.48 g, 81%). $^1\text{H-NMR}$ (400 MHz, Chloroform-*d*) δ 7.82 (d, J = 4.0 Hz, 2H), 7.18 (d, J = 4.1 Hz, 2H), 4.64 (d, J = 6.7 Hz, 2H), 2.23 (p, J = 6.2 Hz, 1H), 1.32-1.21 (m, 24H), 0.87 (m, 6H). $^{13}\text{C-NMR}$ (101 MHz, Chloroform-*d*) δ 141.8, 136.6, 132.1, 129.7, 129.2, 122.8, 115.9, 60.3, 39.2, 32.0, 31.9, 31.5, 31.4, 30.0, 29.7, 29.6, 29.4, 26.3, 26.2, 22.8, 22.7, 14.2, 14.2.

Polymerization of J101. In a dry 50 mL two-necked flask, M1 (111.9 mg, 0.15 mmol) and M2 (148.9 mg, 0.15 mmol) were dissolved in 10 mL dry toluene. After flushing with argon for 10 minutes, 7.6 mg of Pd(PPh₃)₄ was added into the flask quickly, the mixture was flushed with argon for another 5 minutes and stirred at 110 °C for 17 hours under argon. Then the reaction mixture was cooled down to room temperature and precipitated into 200 mL of methanol. The polymer was collected by filtration through a Soxhlet extractor and then subjected to soxhlet extractions with methanol, hexane, acetone, and chloroform each for 12 hours, respectively. Then the chloroform fraction was concentrated and precipitated with methanol, the purple-black solid was obtained. Yield: 140 mg (53.7%). HT-GPC: M_w = 53.3 kDa ; M_n = 28.1 kDa; PDI = 1.90.

Instruments and measurements

$^1\text{H-NMR}$ and $^{13}\text{C-NMR}$ spectra were recorded on a Bruker AVANCE 300 MHz or 400 MHz NMR spectrometer at room temperature. The molecular weight of the polymers was estimated by high-temperature gel permeation chromatography (HT-GPC) using 1,2,4-trichlorobenzene (TCB) as the eluent at 160 °C and monodispersed polystyrene as the standard. We calculated the twisting barriers between benzotriazole and thiophene in 2ClBTz-T and 2FBTz-T by density

functional theory at the B3LYP/6-31G (d, p) level.^{2,3}

Absorption profiles were recorded with a Perkin Elmer Lambda-35 absorption spectrometer from 300 nm to 900 nm. Electrochemical properties were studied by cyclic voltammetry (CV). CV was performed on a CS350H electrochemical workstation with a three-electrode system in a 0.1 M [Bu₄N]PF₆ acetonitrile solution at a scan rate of 10 mV s⁻¹. Glassy carbon disc coated with sample film was used as the working electrode. A Pt wire was used as the counter electrode and Ag/AgCl was used as the reference electrode. The HOMO and LUMO levels are calculated from the onset potentials of oxidation and reduction with respect to the energy level of ferrocene/ferrocenium couple, which was taken as -4.8 eV below the vacuum level

AFM measurements were performed with a Nano Wizard 4 atomic force microscopy (JPK Inc. Germany) in Qi mode to observe the surface morphologies of the J71:ZITI and J101:ZITI (as-cast and annealed) films deposited on glass substrates. TEM was performed on the FEI TITAN3 Themis 60-300 double aberration-corrected microscope at the Shenzhen Cauchy data Co. Ltd, equipped with the super-X energy dispersive spectrometer. 2D GIWAXS measurements: The 2D GIWAXS measurement was performed at the small and wide angle X-ray scattering beamline at the Australian Synchrotron. A Pilatus 1M 2-dimensional detector with 0.172 mm × 0.172 mm active pixels was utilized in integration mode. The detector was positioned approximately 300 mm downstream from the sample location. The precise sample-to-detector distance was determined with a silver behenate standard. 11 KeV incident X-ray with approximately a 0.25 mm × 0.1 mm spot was used to provide large enough q space. The 2-dimensional raw data was reduced and analyzed with a modified version of Nika. 1D GIWAXS patterns shown have been corrected to represent real Q_z and Q_{xy} axes with the consideration of missing wedge. Critical incident angle was determined by the maximized scattering intensity from sample scattering with negligible contribution from underneath layer scattering. The shallow incident angle scattering was collected at 0.02°, which renders the incident X-ray as an evanescent wave along the top surface of thin films.

SCLC measurement: Single carrier devices were fabricated and the dark current-voltage characteristics measured and analyzed in the space charge limited current (SCLC) regime following the references. The structure of hole only devices was Glass/ITO/PEDOT:PSS/Active layer/MoO₃/Ag (100 nm). For the electron only devices, the structure was Glass/ITO/ZnO/Active layer/Ca (15 nm)/Ag (80 nm), where both Ca and Ag were evaporated. The reported mobility data are average values over the two cells of each sample at a given film composition.

Photo-CELIV measurement: In photo-CELIV measurements, the devices were illuminated with a 405 nm laser diode. Current transients were recorded across the internal 50 resistors of our oscilloscope. Here, a fast electrical switch was used to isolate the device, in order to prevent carrier extraction or sweep out. After the variable delay time, the switch connected the device to a function generator. It applied a linear extraction ramp, which was 50 us long and 10.0 V high. Moreover, it started with an offset matching the V_{oc} of the device for each delay time.

TPV and CE measurements: In the TPV measurements, a 405 nm laser diode was used to keep the organic solar cells in the V_{oc} conditions. Measuring the light intensity with a highly linear photodiode and driving the laser intensity with a waveform generator (Agilent 33500B) allowed reproducible adjustments of the light intensities over a range from 0.2 to 2 suns. Moreover, a small perturbation was induced with a second 405 nm laser diode. The intensity of the short laser pulse was adjusted to keep the voltage perturbation below 10 mV. After the pulse, the voltage decays back to its steady state value in a single exponential decay. In the CE measurements, a 405 nm laser diode also illuminated the organic solar cells, which was sufficient to reach a constant V_{oc} with the steady state conditions. At the end of the illumination period, an analogue switch was triggered that switched the device from open-circuit to short-circuit (50Ω) conditions within less than 50 ns.

Fabrication and characterization of the PSCs. All the devices were fabricated in the normal

architecture. These substrates were cleaned in toluene, water, acetone, and isopropyl alcohol. After drying, the substrates were spin-coated with 40 nm PEDOT:PSS (HC Starck, PEDOT PH-4083). The photovoltaic layers were spin-coated in a glovebox from a solution of J101: acceptors with 16 mg mL⁻¹ in chloroform. A perylene diimide functionalized with amino *N*-oxide (PDINO) layer via a solution concentration of 1.0 mg mL⁻¹ was deposited the top of the active layer. Finally, the top aluminum electrode of 100 nm thickness was evaporated in a vacuum onto the cathode buffer layer at a pressure of 5×10^{-6} mbar. The typical active area of the investigated devices was 4 mm². The current-voltage characteristics of the solar cells were measured by a Keithley 2400 source meter unit under AM1.5G (100 mW cm⁻²) irradiation from a solar simulator (Enlitech model SS-F5-3A). Solar simulator illumination intensity was determined at 100 mW cm⁻² using a monocrystalline silicon reference cell with KG5 filter. Short circuit currents under AM1.5G (100 mW cm⁻²) conditions were estimated from the spectral response and convolution with the solar spectrum. The external quantum efficiency was measured by a Solar Cell Spectral Response Measurement System QE-R3011(Enli Technology Co., Ltd.).

Experimental data

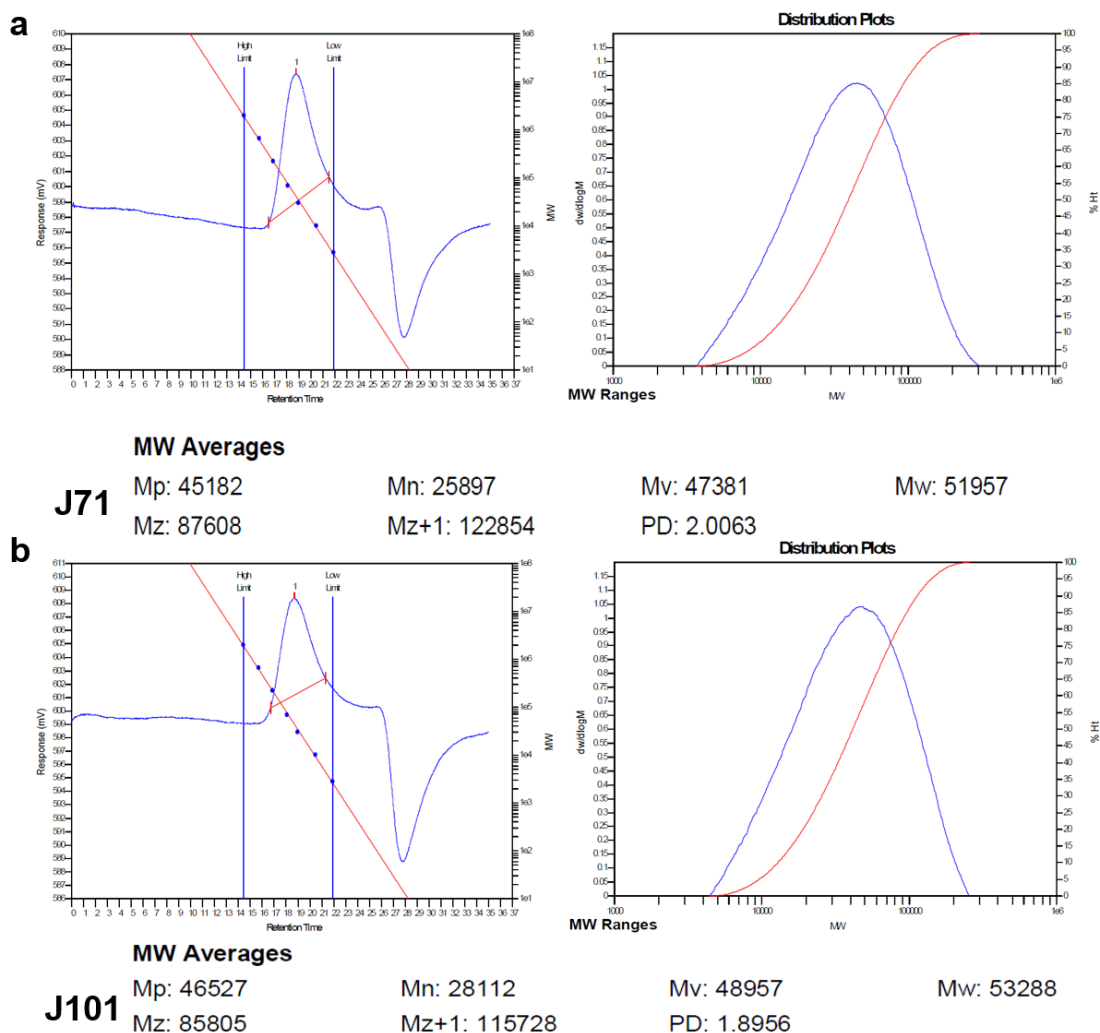


Figure S1. The HT-GPC diagrams of a) J71 and b) J101 using trichlorobenzene as eluent.

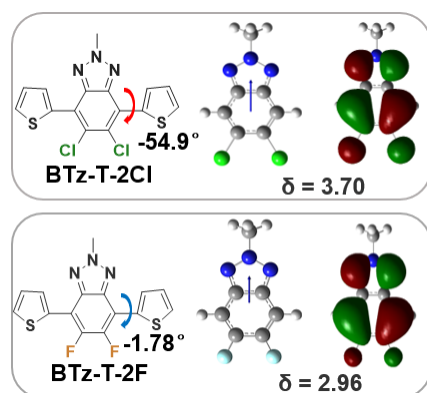


Figure S2. The twisting effects in two BTz units, the dipole moments and HOMO surfaces in the BTz-T-2Cl and BTz-T-2F.

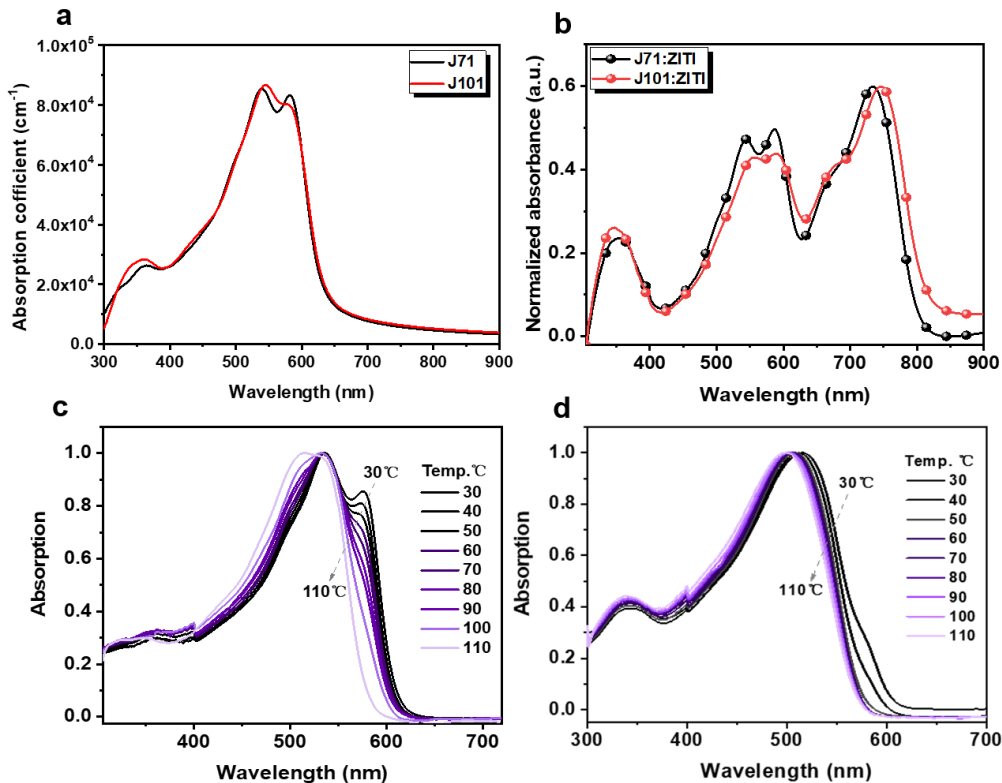


Figure S3. a) Absorption coefficients of J101 and J71 film. b) Normalized absorption spectra of the blend films of J71:ZITI and J101:ZITI. Temperature-dependent absorption (TD-Abs) spectra of c) J71 and d) J101 in *o*-DCB dilute solutions as the temperature decreased from 30 to 110 °C.

Table S1. Molecular weights, optical and electrochemical properties of J101 and J71.

polymers	M_n [kDa]	PDI $[M_w/M_n]$	λ_{max} [nm] ^a	λ_{edge} [nm] ^b	E_g^{opt} [eV] ^c	E_{HOMO} [eV] ^d	E_{LUMO} [eV] ^d	E_g^{ec} [eV] ^e
J101	28.1	1.89	544, 581	631	1.965	-5.30	-3.50	1.80
J71	25.9	2.00	539, 580	628	1.975	-5.27	-3.60	1.67

^aThin films of J101 and J71 on quartz plate cast from chloroform solution. ^babsorption edge of J101 and J71 films. ^cCalculated from the absorption edge of J101 and J71 films: $E_g^{\text{opt}} = 1240/\lambda_{\text{edge}}$. ^dMeasured by cyclic voltammetry and calculated according to the equation: $E_{\text{HOMO/LUMO}} = -e(E_{\text{ox/red}} + 4.40)$ (eV). ^eElectrochemical bandgap obtained from $E_{\text{LUMO}} - E_{\text{HOMO}}$.

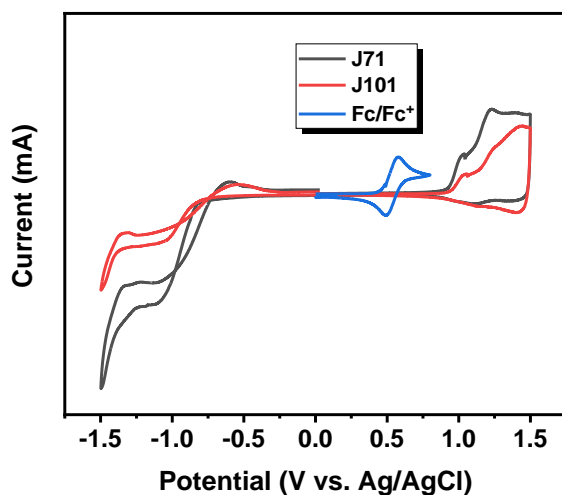


Figure S4. Cyclic voltammograms of J71 (black line), J101 (red line) and ferrocene/ferrocenium (Fc/Fc^+ , blue line).

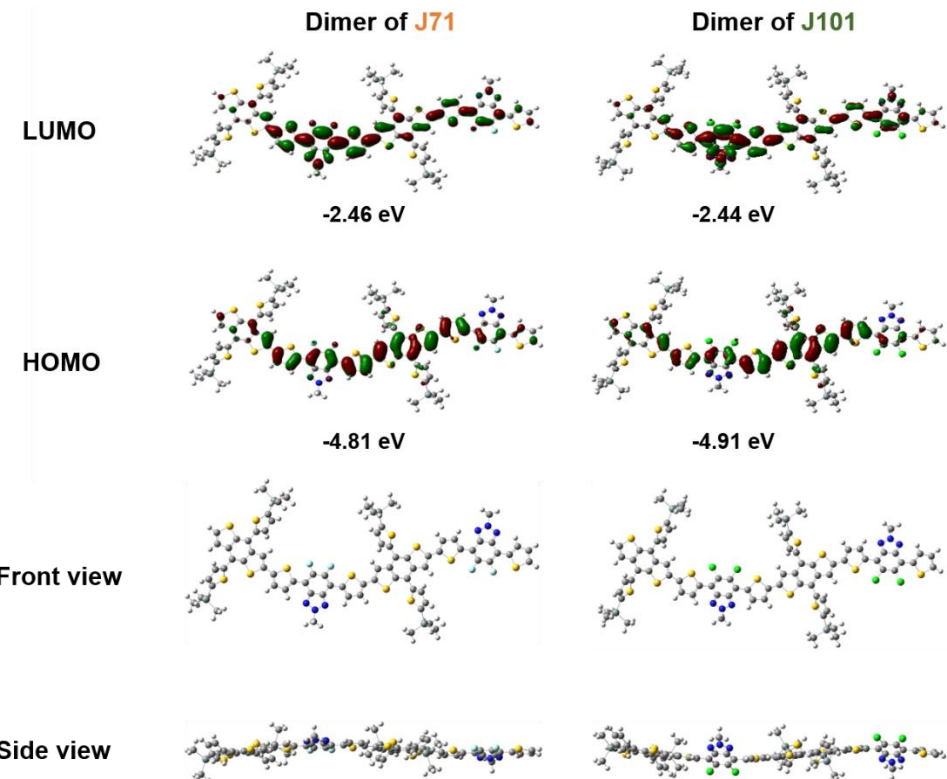


Figure S5. Simulated molecular geometries. The LUMO and HOMO electron density distribution and energy levels of dimers of J101 and J71 by DFT calculations at the B3LYP/6-31G (d, p) level. To simplify the calculations, alkyl chains were replaced by methyl groups. The S atoms are marked in yellow, N atoms are shown in blue, Cl atoms are marked in green, F atoms are marked in cyan, C atoms are shown in gray, and H atoms are marked in white.

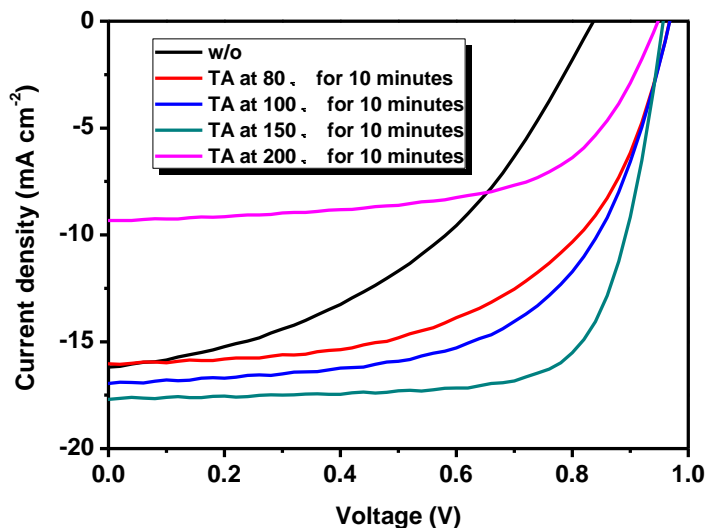


Figure S6. $J-V$ curves of devices based on J101:ITIC films with different thermal annealing temperature under the illumination of an AM 1.5G solar simulator, 100 mW cm^{-2} .

Table S2. Photovoltaic parameters of devices based on J101:ITIC films with different TA temperature under the illumination of an AM 1.5G solar simulator, 100 mW cm^{-2} .

Temperature [°C]	V_{oc} [V]	J_{sc} [mA cm $^{-2}$]	FF [%]	PCE (PCE a) [%]
w/o	0.836	16.19	43.49	5.89 (5.64)
80	0.968	16.03	56.55	9.77 (9.56)
100	0.968	16.95	60.17	9.87 (9.76)
150	0.951	17.69	73.65	12.47 (12.23)
200	0.948	9.32	61.29	5.42 (5.25)

a The values in square bracket are the average PCE obtained from six devices.

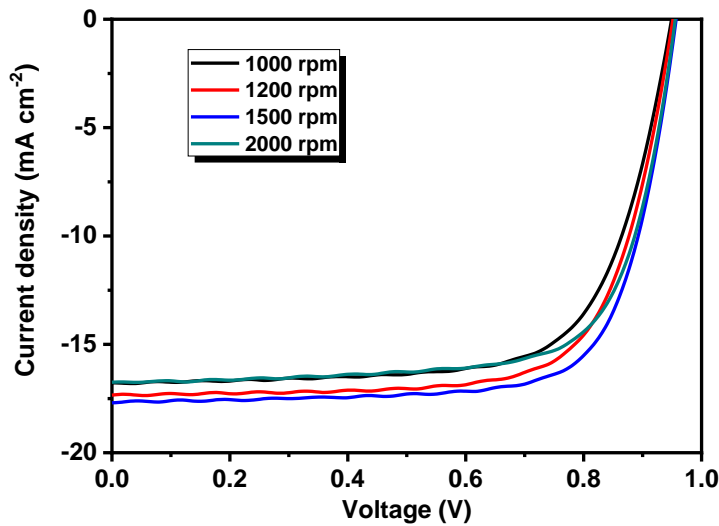


Figure S7. J - V curves of devices based on J101:ITIC films with different coating speeds (thermal annealing at $150 \text{ }^\circ\text{C}$ for 10 minutes) under the illumination of an AM 1.5G solar simulator, 100 mW cm^{-2} .

Table S3. Photovoltaic parameters of devices based on J101:ITIC films with different coating speeds (thermal annealing at $150 \text{ }^\circ\text{C}$ for 10 minutes) under the illumination of an AM 1.5G solar simulator, 100 mW cm^{-2} .

Speed[rpm]/ Thickness [nm]	V_{oc} [V]	J_{sc} [mA cm $^{-2}$]	FF [%]	PCE (PCE a) [%]
1000/130	0.949	16.77	70.12	11.16 (11.02)
1200/112	0.951	17.34	71.80	11.84 (11.53)
1500/98	0.951	17.69	73.65	12.47 (12.23)
2000/86	0.955	16.74	72.29	11.56 (11.12)

a The values in square bracket are the average PCE obtained from six devices.

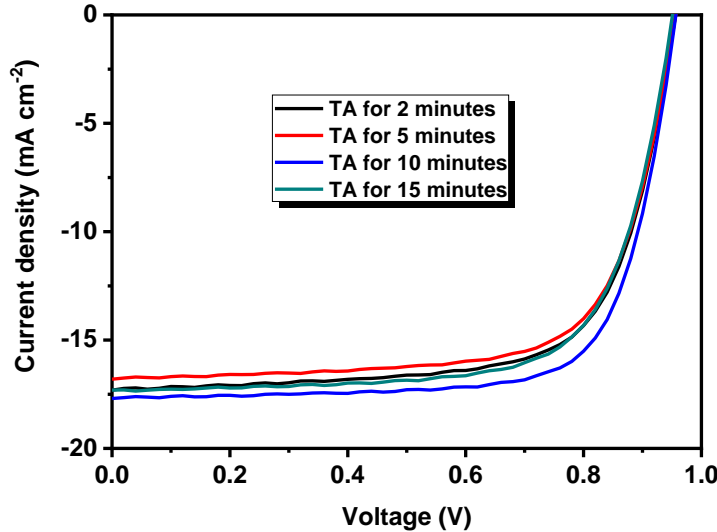


Figure S8. J - V curves of devices based on J101:ITIC films with different thermal annealing time at 150 °C under the illumination of an AM 1.5G solar simulator, 100 mW cm⁻².

Table S4. Photovoltaic parameters of devices based on J101:ITIC films with different thermal annealing time at 150 °C under the illumination of an AM 1.5G solar simulator, 100 mW cm⁻².

Time [minutes]	V_{oc} [V]	J_{sc} [mA cm ⁻²]	FF [%]	PCE (PCE ^a) [%]
2	0.956	17.32	70.03	11.59 (11.20)
5	0.956	16.81	70.36	11.31 (11.12)
10	0.951	17.69	73.65	12.47 (12.23)
15	0.951	17.31	70.74	11.64 (11.34)

^aThe values in square bracket are the average PCE obtained from six devices.

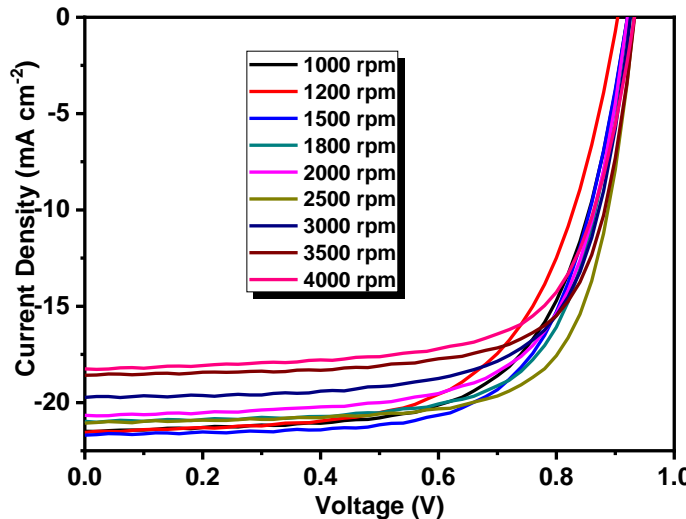


Figure S9. J - V curves of devices based on J101:ZITI films with different coating speeds under the illumination of an AM 1.5G solar simulator, 100 mW cm⁻².

Table S5. Photovoltaic parameters of devices based on J101:ZITI films with different coating speeds and thermal annealing at 150 °C for 2 minutes under the illumination of an AM 1.5G solar simulator, 100 mW cm⁻².

Speed[rpm]/ Thickness[nm]	V _{oc} [V]	J _{sc} [mA cm ⁻²]	FF [%]	PCE (PCE ^a) [%]
1000/169	0.920	21.49	66.00	13.06 (12.89)
1200/158	0.904	21.54	62.85	12.25 (12.02)
1500/140	0.921	21.68	67.78	13.53 (13.34)
1800/125	0.920	20.96	70.38	13.60 (13.40)
2000/114	0.921	20.66	68.51	13.02 (12.78)
2500/105	0.937	21.25	72.48	14.43 (14.12)
3000/94	0.926	19.73	69.69	12.73 (12.56)
3500/84	0.933	18.58	72.00	12.48 (12.22)
4000/76	0.932	18.25	69.28	11.79 (11.46)

^aThe values in square bracket are the average PCE obtained from six devices.

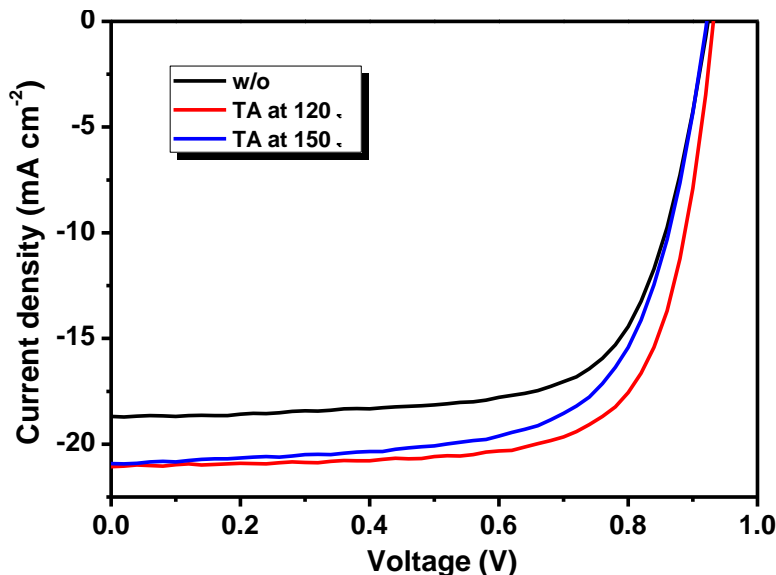


Figure S10. J-V curves of devices based on J101:ZITI films with different thermal annealing temperature under the illumination of an AM 1.5G solar simulator, 100 mW cm⁻².

Table S6. Photovoltaic parameters of devices based on J101:ZITI films with different TA temperature under the illumination of an AM 1.5G solar simulator, 100 mW cm⁻².

Temperature [°C]	V _{oc} [V]	J _{sc} [mA cm ⁻²]	FF [%]	PCE (PCE ^a) [%]
w/o	0.926	19.79	69.08	12.67 (12.34)
120	0.937	21.25	72.48	14.43 (14.12)
150	0.922	20.91	68.21	13.14 (12.88)

^aThe values in square bracket are the average PCE obtained from six devices.

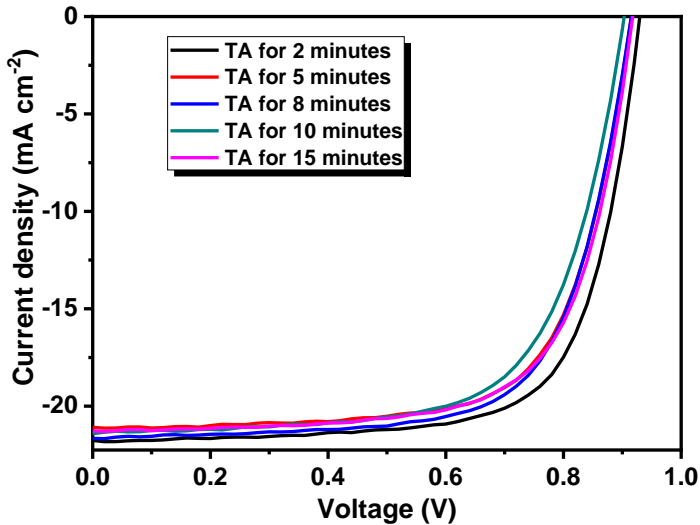


Figure S11. J - V curves of devices based on J101:ZITI films with different thermal annealing time under the illumination of an AM 1.5G solar simulator, 100 mW cm^{-2} .

Table S7. Photovoltaic parameters of devices based on J101:ZITI films with different thermal annealing time under the illumination of an AM 1.5G solar simulator, 100 mW cm^{-2} .

Time [minutes]	V_{oc} [V]	J_{sc} [mA cm $^{-2}$]	FF [%]	PCE (PCE a) [%]
2	0.937	21.25	72.48	14.43 (14.12)
5	0.916	21.09	69.59	13.43 (13.22)
8	0.915	21.65	68.93	13.66 (13.34)
10	0.903	21.40	66.94	12.94 (12.67)
15	0.917	21.26	68.93	13.45 (13.24)

a The values in square bracket are the average PCE obtained from six devices.

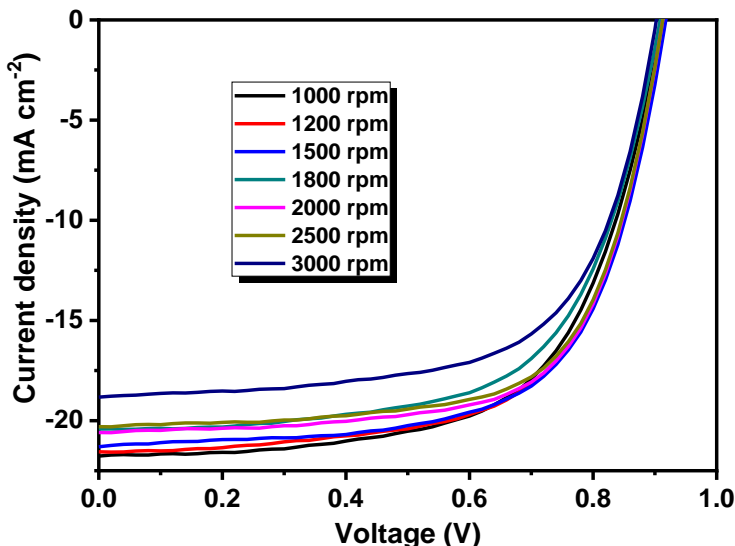


Figure S12. J - V curves of devices based on J71:ZITI films with different coating speeds under the illumination of an AM 1.5G solar simulator, 100 mW cm^{-2} .

Table S8. Photovoltaic parameters of devices based on J71:ZITI films with different coating speeds and thermal annealing at 120 °C for 10 minutes under the illumination of an AM 1.5G solar simulator, 100 mW cm⁻².

Speed[rpm]/Thickness[nm]	V _{oc} [V]	J _{sc} [mA cm ⁻²]	FF[%]	PCE (PCE ^a)[%]
1000/148	0.913	21.77	63.13	12.55 (12.34)
1200/142	0.916	21.55	64.39	12.72 (12.58)
1500/130	0.917	21.3	65.50	12.80 (12.63)
1800/118	0.908	20.42	63.79	11.84 (11.57)
2000/110	0.912	20.59	67.52	12.69 (12.48)
2500/98	0.912	20.23	69.49	12.82 (12.68)
3000/80	0.902	18.83	64.56	10.97 (10.82)

^aThe values in square bracket are the average PCE obtained from six devices.

Table S9. The PCEs for various BTz-based PSCs.

D:A	PCE (%)	References
FTAZ:F9IC	11.7	⁴
PTAZDCB20:PC ₇₁ BM	9.02	⁵
4'-FT-FTAZ:PC ₆₁ BM	8.1	⁶
FTAZ/INIC3	11.5	⁷
FTAZ:PCBM	7.49	⁸
J52:ITIC	5.51	⁹
J60:ITIC	8.97	⁹
J61:ITIC	9.53	⁹
J61:m-ITIC	11.77	¹⁰
J51:N2200	8.27	¹¹
J50:ITIC	4.8	¹²
J51:ITIC	9.26	¹²
J71:ITIC	11.41	¹³
J81:ITIC	10.6	¹⁴
J81:m-ITIC	11.05	¹⁴
J91:m-ITIC	11.63	¹⁵
J52:m-ITIC	5.98	¹⁵
J71:ZITI	13.28	¹⁶
J61:BT-IC	9.56	¹⁷
J71:BT-IC	10.46	¹⁷
PBTA-BO:IFBR:PC ₆₁ BM	8.11	¹⁸
J52:IT-M	9.4	¹⁹
J52:IEICO	6.5	¹⁹
J52:IT-M:IEICO	11.1	¹⁹
FTAZ:ITIC1	8.54	²⁰
FTAZ:ITIC2	11	²⁰
J61-F:ITIC	8.24	²¹
FTAZ:IT-M	11	²²
FTAZ:IDIC	10.4	²³
J51:IDTIDSe-IC	8.02	²⁴
J71:MeIC	12.54	²⁵
FTAZ:ITIC-Th	8.88	²⁶

FTAZ:ITIC-Th1	12.1	26
FTAZ:PC ₇₁ BM	5.22	26
FTAZ:ITIC-Th2	9.06	27
FTAZ:ITIC-Th3	10.7	27
PBnDT-HTAZ:PC ₆₁ BM	4.36	28
PBnDT-FTAZ:PC ₆₁ BM	7.1	28
FTAZ:PC ₆₁ BM	5.93	29
PrzTAZ:PC ₆₁ BM	5	29
PyCNTAZ:PC ₆₁ BM	7.78	29
CNTAZ:PC ₆₁ BM	5.92	29
PBDT-HBTA:PC ₇₀ BM	2.43	30
PBDT-FBTA:PC ₇₀ BM	6	30
PBDTTDTBT:PC ₇₁ BM	3.1	31
PBDTDTBTz : PC ₆₁ BM	1.5	32
PBDTDTBTz : PC ₇₁ BM	1.7	32
PBDTB TZ : PC ₆₁ BM	0.7	32
PBDTB TZ : PC ₇₁ BM	1.4	32
PBDT-DTBTz:PC ₇₁ BM	2.88	33
PTIPSBDTDTBTz:PC ₇₁ BM	5.53	33
PT4Si-FTAZ:ITIC	6.79	34
PBDTSi-TA:ITIC	7.51	35
S-PBDTB TZ:PC ₇₁ BM	5.5	36
A-PBDTB TZ:PC ₇₁ BM	3.2	36
F-PBDTB TZ:PC ₇₁ BM	2.7	36
PHTBT:PCBM	0.33	37
PF-DTBTBTA:PCBM	1.3	38
PCz-DBTA:PCBM	2.75	38
PPh-DBTA:PCBM	1.39	38
J62:ITIC	10.81	39
J63:ITIC	8.13	39
J64:ITIC	8.59	39
PBDT-TAZ:NOE0	6.8	40
PBDT-TAZ:NOE10	8.1	40
PBDT-TAZ:NOE20	7.3	40
PBDT-TAZ:NOE30	6.1	40
J70:m-ITIC	11.62	41
J71:m-ITIC	12.05	41
J72:m-ITIC	10.23	41
J73:m-ITIC	10.71	41
J74:m-ITIC	9.63	41
J71:IDTT-BH	11.05	42
J71:IDTT-OBH	8.02	42
PfBT AZ:O-IDTBR	7.7	43
PfBT AZS:O-IDTBR	10.4	43
PBDFS-Bz:ITIC	8.07	44
PBDFS-fBz:ITIC	9	44
J61:ICTP	3.24	45
J51: IDSe-T-IC	8.21	46
J51: PC ₇₁ BM	6	46

J52:BTA13	7.82	47
J52-F:BTA13	8.36	47
J52-FS:BTA13	3.84	47
J61:SJ-IC	9.27	48
J61:IDT-IC	6.95	48
J71:ITIC1	8.99	49
J71:ITIC5	12.5	49
PTBFBz:ITIC	8.33	50
PBDTBz:ITIC	5.51	50
J61:ITIC	9.32	51
PvBDTTAZ:O-IDTBR	11.6	52
FTAZ>NNFA[0, 6]	9.52	53
FTAZ>NNFA[6, 3]	7.56	53
FTAZ>NNFA[6, 6]	10.56	53
FTAZ>NNFA[12, 3]	10.81	53
FTAZ>NNFA[12, 6]	9.54	53
FTAZ:IDIC1	7.13	54
FTAZ:IHIC1	9.21	54
FTAZ:IDIC	12.5	55
FTAZ:IDIC	12.91	56
J71:IT-IC	9	57
J71:BDT-IC	10.05	57
FTAZ:COi6IC	8.43	58
FTAZ:COi6FIC	9.12	58
FTAZ:COi6DFIC	8.25	58
FTAZ:IHIC2	7.45	59
FTAZ:IOIC2	12.3	59
J71:m-MeIC	12.08	60
PBT1Cl-Bz:IT-4F	7.6	61
PBT2Cl-Bz:IT-4F	7.8	61
PBT4Cl-Bz:IT-4F	9.25	61
J101:ITIC	12.47	This work
J101:ZITI	14.43	This work

Table S10. PCE (%), E_g^{opt} (eV), V_{OC} (V), and E_{loss} (eV) for various PSCs.

Donor	Acceptor	PCE (%)	E_g^{opt} (eV)	V_{oc} (V)	E_{loss} (eV)	References
PBDB-T	IT-M	12.05	1.6	0.94	0.66	62
PBDB-T	IT-DM	11.29	1.63	0.97	0.63	62
PBDT-TDZ:ITIC	ITIC	11.72	1.58	1.01	0.57	63
PBDTS-TDZ:ITIC	ITIC	12.8	1.58	1.1	0.48	63
PffQx-T	ITIC	8.47	1.57	0.87	0.7	64
PffQx-PS	ITIC	9.12	1.57	0.97	0.6	64
PffQx-T	PC ₇₁ BM	8.3	1.73	0.86	0.87	64
PffQx-PS	PC ₇₁ BM	8	1.81	0.93	0.88	64
J52	ITIC	5.51	1.57	0.73	0.84	9
J60	ITIC	8.97	1.57	0.91	0.66	9

J61	ITIC	9.53	1.57	0.89	0.68	9
PBD1	PC ₇₁ BM	9.8	1.88	0.91	0.97	65
PBDTTT-E-T	IEICO	8.4	1.34	0.82	0.52	66
PBDTTT-E-T	IEIC	4.9	1.5	0.9	0.6	66
PBDB-T-SF	IT-4F	13.1	1.54	0.88	0.66	67
PBDTTT-C-T	DC-IDT2T	3.93	1.55	0.9	0.65	68
PTB7-TH	IEIC	6.31	1.57	0.97	0.6	69
PM6	IDTN	12.2	1.59	0.946	0.644	70
PTB7-Th	ATT-1	10.07	1.54	0.87	0.67	71
P3HT	O-IDTBR	6.4	1.63	0.73	0.9	72
P3HT	EH-IDTBR	6	1.68	0.82	0.86	72
PBDB-T	NTIC	8.63	1.67	0.935	0.735	73
PBDB-T	NTIC-Me	8.3	1.74	0.963	0.777	73
PBDB-T	NTIC-OMe	8.61	1.71	0.965	0.745	73
PBDB-T	NTIC-F	8.1	1.66	0.812	0.848	73
PTB7-Th	IHIC	9.77	1.38	0.754	0.626	74
PDBT-T1	IC-C6IDT-IC	8.71	1.62	0.89	0.73	75
PTB7-Th	ITIC	6.8	1.59	0.81	0.78	76
J71	BT-IC	10.28	1.43	0.9	0.53	17
J61	<i>m</i> -ITIC	11.77	1.58	0.912	0.668	10
PTB7-Th	CO _i 8DFIC	12.16	1.26	0.68	0.58	77
PTB7-Th	IEICO-4Cl	10.3	1.23	0.727	0.503	78
TQ1	PC ₇₁ BM	5.8	1.7	0.91	0.79	79
PTB7	PC ₇₁ BM	7.4	1.6	0.74	0.86	80
J51	N2200	8.27	1.48	0.83	0.65	11
PNDTDPP	PC ₇₁ BM	6.92	1.36	0.76	0.6	81
FTAZ	INIC	7.7	1.57	0.96	0.61	7
FTAZ	INIC1	10.1	1.56	0.93	0.63	7
FTAZ	INIC2	10.6	1.52	0.9	0.62	7
FTAZ	INIC3	11.2	1.48	0.86	0.62	7
J71	ITIC	11.41	1.59	0.96	0.63	13
PffBT-T4-2HD	PC ₇₁ BM	7	1.65	0.73	0.92	82
PffBT-T3(1,3)	PC ₇₁ BM	3.7	1.6	0.77	0.83	82
PffBT-T3(1,2)-1	PC ₇₁ BM	9.7	1.63	0.82	0.81	82
PffBT-T3(1,2)-2	PC ₇₁ BM	10.5	1.63	0.82	0.81	82
PffBT-T2	PC ₇₁ BM	4.3	1.61	0.88	0.73	82
PDBT-T1	PC ₇₀ BM	9.74	1.85	0.92	0.93	83
PDBT-T1	SdiPBI-Se	8.42	1.85	0.947	0.903	84
PBDB-T	ITCC	11.4	1.67	1.01	0.66	85
PTB7-Th	FNIC1	10.3	1.48	0.774	0.706	86
PTB7-Th	FNIC2	13	1.38	0.741	0.639	86
HFAQx-T	PC ₇₁ BM	9.2	1.73	0.9	0.83	87
P1	IT-4F	11.5	1.52	0.896	0.624	88
P2	IT-4F	14.2	1.52	0.9	0.62	88
P3	IT-4F	11.2	1.52	0.904	0.616	88

PDTP-DFBT	PC ₇₁ BM	8	1.38	0.698	0.682	89
PDTTDPP	PC ₇₁ BM	6.05	1.22	0.66	0.56	90
PBDB-T	NITI	12.74	1.49	0.86	0.63	91
PTB7-Th	DICTF	7.93	1.82	0.85	0.97	92
P3HT	N5	2.76	2.2	0.78	1.42	93
PBDB-T	DF-PCIC	10.14	1.59	0.91	0.68	94
PCPDTBT	PC ₇₁ BM	5.5	1.46	0.62	0.84	95
PTB7	PDI1	5.14	1.65	0.79	0.86	96
PTB7-Th	PDIBDT-RDN	3.34	1.64	0.76	0.88	97
PTB7-Th	PDIBDT-IT	6.06	1.69	0.74	0.95	97
PTB7-Th	PDIBDT-ITF	4.67	1.68	0.71	0.97	97
PIPCP	PC ₆₁ BM	6.13	1.47	0.86	0.61	98
PBDB-T	FDICTF	10	1.63	0.94	0.69	99
PBDB-T	FDNCTF	11.2	1.6	0.93	0.67	99
PTB7	hPDI3	6.4	1.65	0.77	0.88	100
PTB7-Th	hPDI3	7.9	1.58	0.81	0.77	100
PTB7	hPDI4	6.5	1.65	0.78	0.87	100
PTB7-Th	hPDI4	8.3	1.58	0.8	0.78	100
PSEHTT	DBFI-DMT	6.37	1.87	0.92	0.95	101
PSEHTT	DBFI-S	2.61	1.87	0.82	1.05	101
PSEHTT	DBFI-MTT	3.94	1.87	0.94	0.93	101
PffBT4T-2OD	PC ₇₁ BM	10.8	1.56	0.77	0.79	102
PBT1-EH	ITCPTC	11.8	1.58	0.95	0.63	103
PBT1-EH	ITIC	9.8	1.6	0.99	0.61	103
PNOz4T	PC ₆₁ BM	8.8	1.52	0.97	0.55	104
PNOz4T	PC ₇₁ BM	8.9	1.52	0.96	0.56	104
PNTz4T	PC ₆₁ BM	8.7	1.56	0.738	0.822	105
PNTz4T	PC ₇₁ BM	8.92	1.56	0.712	0.848	105
J52	IEICO-4F	9.4	1.24	0.734	0.506	106
PBDTTT-EFT	IEICO-4F	10	1.24	0.739	0.501	106
P1	PC ₇₀ BM	5.14	1.8	0.8	1	107
TTV1	PC ₇₀ BM	6.46	1.8	0.78	1.02	107
P2	PC ₇₀ BM	3.48	1.1	0.4	0.71	107
TTV2	PC ₇₀ BM	4.99	1.1	0.42	0.69	107
PDPPTPyT	PC ₆₀ BM	4.5	1.34	0.55	0.79	108
PDPPSPyS	PC ₆₀ BM	3.1	1.24	0.48	0.76	108
PDPPTDTPT	PC ₆₀ BM	3.8	1.23	0.43	0.8	108
PDPPSDTPS	PC ₆₀ BM	2.9	1.13	0.34	0.79	108
PDPP2Tz2T	PC ₇₁ BM	5.1	1.47	0.92	0.55	109
PDPP2TzDTP	PC ₇₁ BM	5.6	1.28	0.69	0.59	109
PBDB-T	IT-OM-1	6.3	1.74	1.01	0.73	110

PBDB-T	IT-OM-2	11.9	1.63	0.93	0.7	¹¹⁰
PBDB-T	IT-OM-3	10.8	1.72	0.97	0.75	¹¹⁰
PBDB-T	IT-OM-4	7.9	1.68	0.96	0.72	¹¹⁰
P1	PY1	4.89	1.4	0.86	0.54	¹¹¹
P1	DCI-2	6.94	1.23	0.8	0.43	¹¹¹
P1	PC ₇₁ BM	5.3	1.6	0.84	0.76	¹¹¹
FTAZ	ITIC-Th	8.88	1.6	0.92	0.68	²⁶
FTAZ	ITIC-Th1	12.1	1.55	0.85	0.7	²⁶
J101	ITIC	12.47	1.57	0.951	0.619	This work
J101	ZITI	14.43	1.53	0.937	0.593	This work

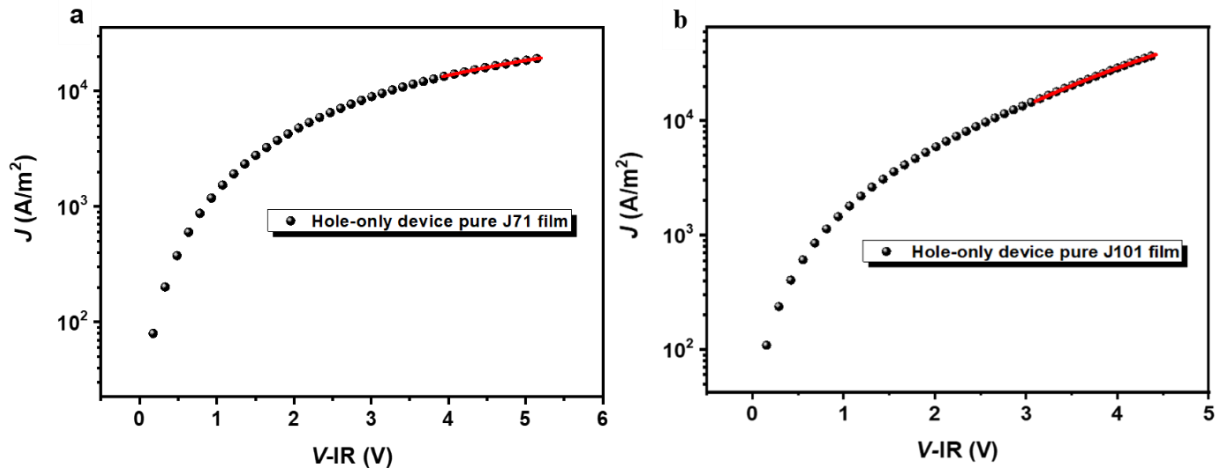


Figure S13. The dark J - V characteristics of hole-only devices for pure J71 a) and J101 films b) (the red solid lines are fitted according to the space-charge-limited current model).

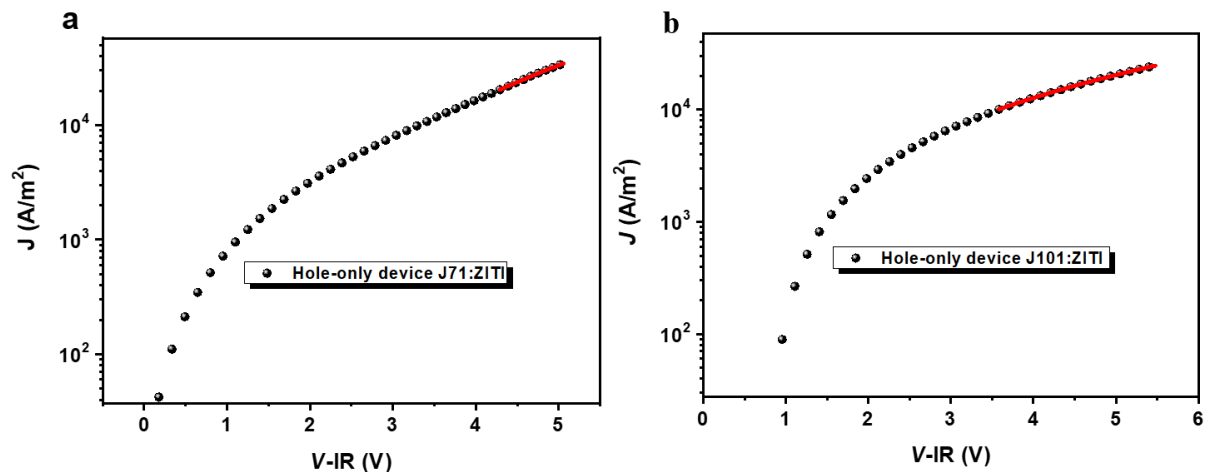
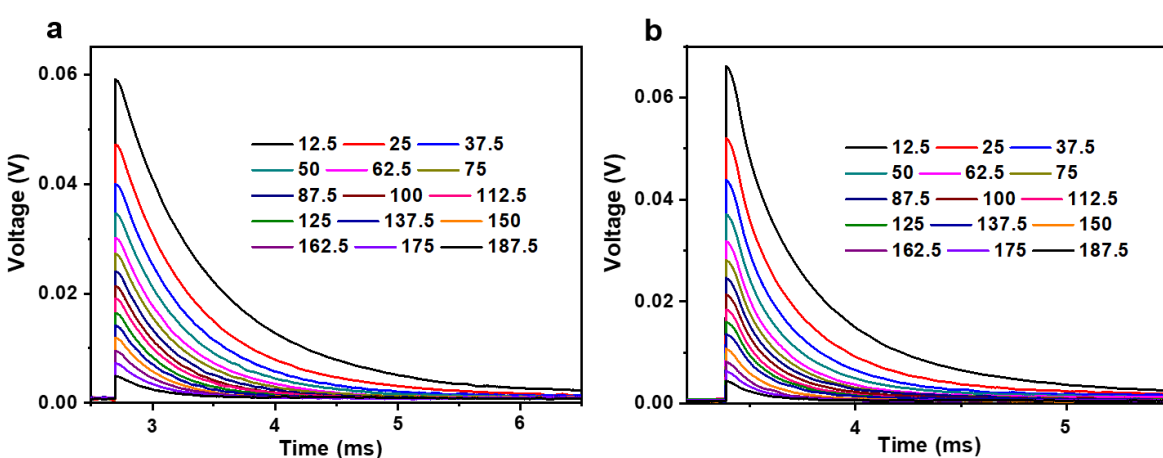
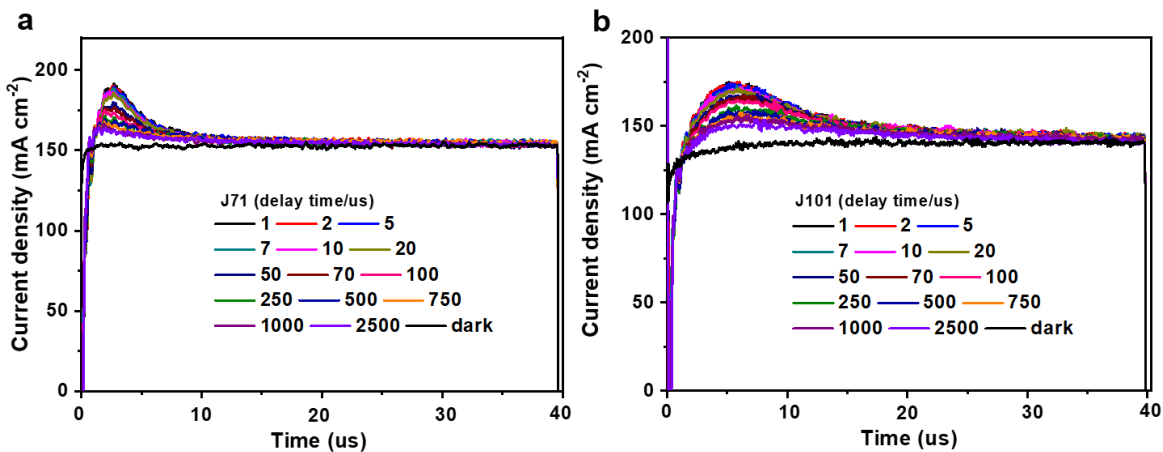
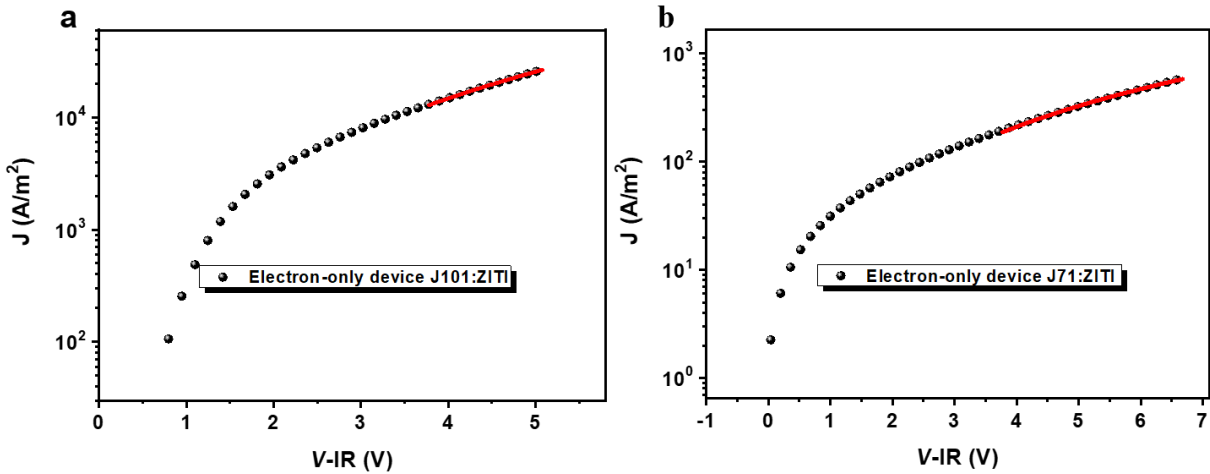


Figure S14. The dark J - V characteristics of hole-only optimized devices for a) J71:ZITI and b) J101:ZITI blend films, (the red solid lines are fitted according to the space-charge-limited current model).



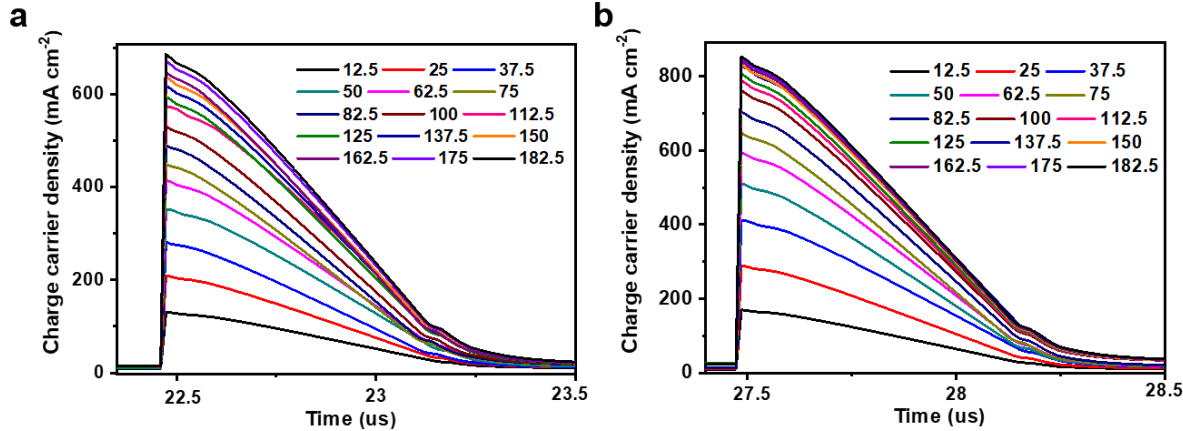


Figure S18. Charge extraction measurements of a) J71:ZITI and b) J101:ZITI solar cells tested in different time periods, respectively. The strong dependence of light intensity and carrier density can be observed.

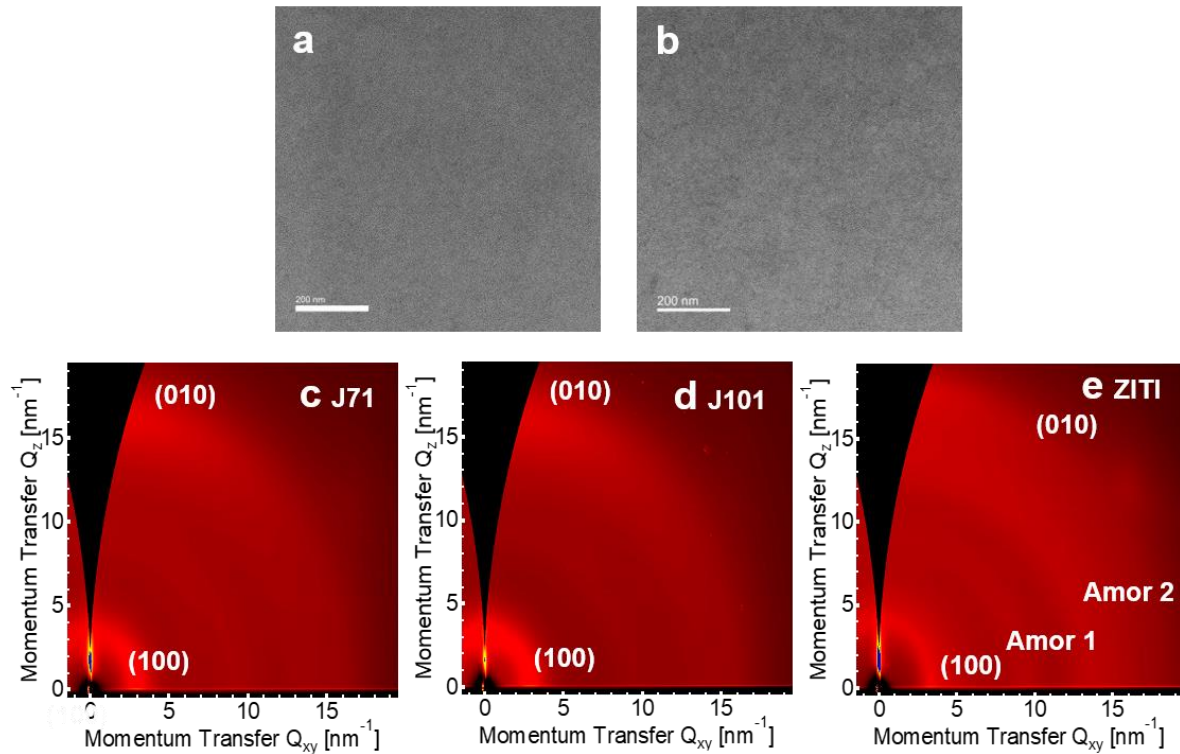


Figure S19. TEM images of a) J71:ZITI, b) J101:ZITI, the scale bars are 200 nm. The 2D GIWAXS images of c) neat J71 film, d) neat J101 film, e) neat ZITI film. The 1D GIWAXS patterns along in-plane and out-of-plane directions of J71, J101, and ZITI neat films are displayed in Figure 4g. The neat films of both polymers exhibited sharp diffraction peaks (100) in the in-plane direction and with a moderate diffraction peak (010) in the out-of-plane direction, indicating the face-on preferential orientation. The (100) lamellar peaks of J71 and J101 are located at $q \approx 0.294$ and 0.291 \AA^{-1} , corresponding to the lamellar spacing of ≈ 21.34 and 21.57 \AA , respectively. Furthermore, in the 2D GIWAXS patterns of the pure J71 and J101 thin films, a medium intensity diffraction peak arises from in the out-of-plane direction ($q \approx 1.61$ and 1.64 \AA^{-1}) and corresponding to the $\pi-\pi$ stacking peaks (≈ 3.90 and 3.83 \AA).

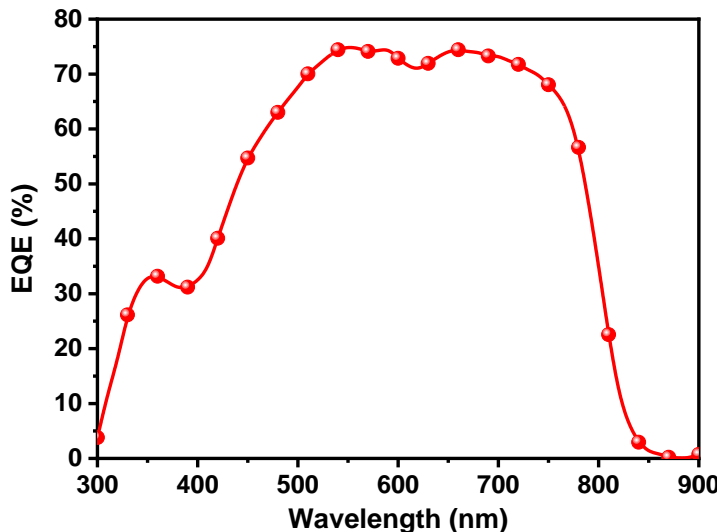


Figure S20. EQE spectra of optimized ST-OSC ($\text{Ag} = 15 \text{ nm}$) device based on J101:ZITI under the illumination of an AM 1.5G solar simulator, 100 mW cm^{-2} .

Table S11. AVT (%) and PCE (%) of some representative single-junction ST-OSCs reported in literature and this work.

AVT (%)	PCE (%)	References
36	9.77	74
25	6	112
30	5.6	113
29.1	3.1	114
22.4	3.3	114
19	3.2	114
27.4	6.1	114
16.3	6.5	114
27.6	5.4	114
16.9	6.4	114
22	5.9	114
32.5	5.8	114
34.1	5.5	114
24.7	2.9	114
12.2	7	114
30	6.1	115
36	6.87	116
50	2.88	117
25.2	7.3	118
37.4	10.3	119
31	10.2	120
26	8.2	121
25.6	8.38	78
35.7	6.24	78
35.1	6.37	78
33.5	6.97	78
37	7.74	122
39.4	5.1	123

47.3	5	123
58	4.5	124
40	3.4	125
24.59	2.6	126
24.35	5.1	126
13.03	5.63	126
31.71	4.22	126
37	5	127
21.69	11.04	This work

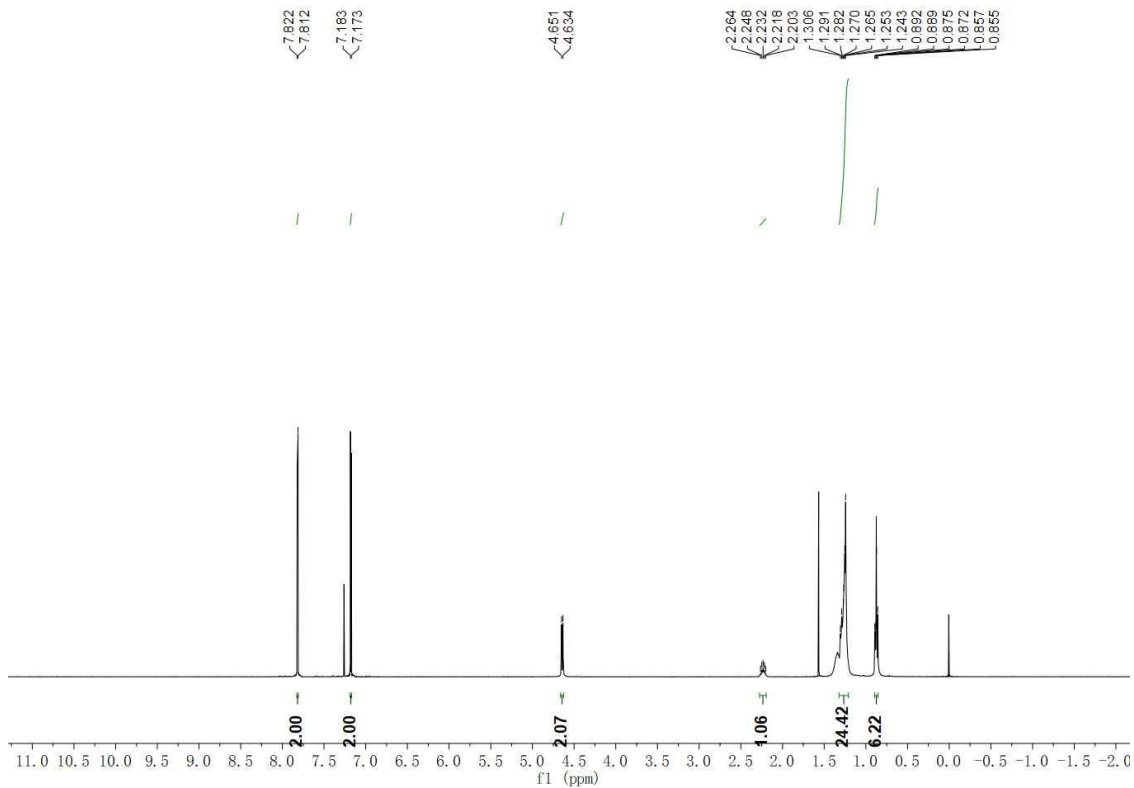


Figure S21. The ^1H -NMR spectra of **M1** in CDCl_3 .

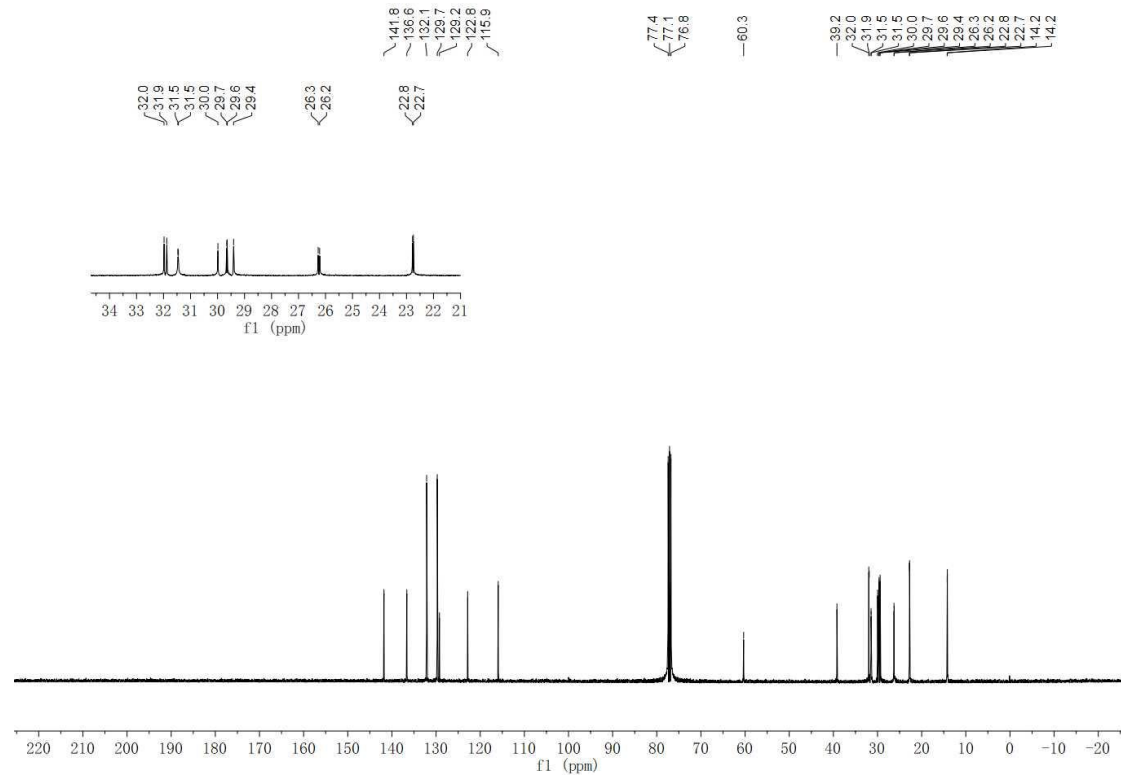


Figure S22. The ^{13}C -NMR spectra of **M1** in CDCl_3 .

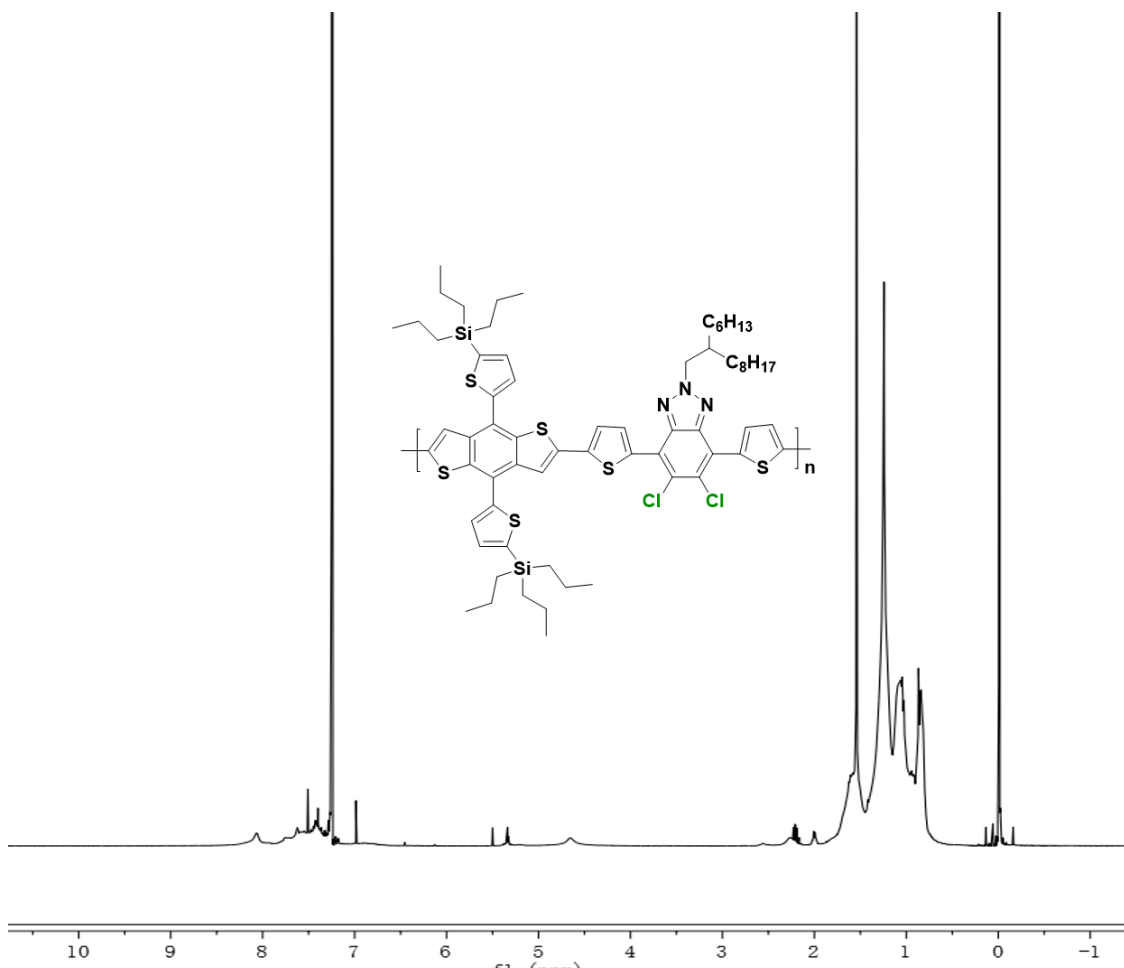


Figure S23. The ^1H -NMR spectra of compound **J101** in CDCl_3 .

References

1. J. Min, Z.-G. Zhang, S. Zhang and Y. Li, *Chem Mater*, 2012, **24**, 3247-3254.
2. S. Q. Zhang, Y. P. Qin, J. Zhu and J. H. Hou, *Adv Mater*, 2018, **30**.
3. S. Zhang, B. Yang, D. Liu, H. Zhang, W. Zhao, Q. Wang, C. He and J. Hou, *Macromolecules*, 2015, **49**, 120-126.
4. S. Dai, Y. Xiao, P. Xue, J. J. Rech, K. Liu, Z. Li, X. Lu, W. You and X. Zhan, *Chem. Mater.*, 2018, **30**, 5390-5396.
5. J. H. Yun, H. Ahn, P. Lee, M. J. Ko and H. J. Son, *Macromolecules*, 2017, **50**, 7567.
6. Q. Zhang, L. Yan, X. Jiao, Z. Peng, S. Liu, J. J. Rech, E. Klump, H. Ade, F. So and W. You, *Chem. Mater.*, 2017, **29**, 5990-6002.
7. S. Dai, F. Zhao, Q. Zhang, T. K. Lau, T. Li, K. Liu, Q. Ling, C. Wang, X. Lu, W. You and X. Zhan, *J. Am. Chem. Soc.*, 2017, **139**, 1336-1343.
8. W. Li, S. Albrecht, L. Yang, S. Roland, J. R. Tumbleston, T. McAfee, L. Yan, M. A. Kelly, H. Ade, D. Neher and W. You, *J. Am. Chem. Soc.*, 2014, **136**, 15566-15576.
9. H. Bin, Z. G. Zhang, L. Gao, S. Chen, L. Zhong, L. Xue, C. Yang and Y. Li, *J. Am. Chem. Soc.*, 2016, **138**, 4657-4664.
10. Y. Yang, Z. G. Zhang, H. Bin, S. Chen, L. Gao, L. Xue, C. Yang and Y. Li, *J. Am. Chem. Soc.*, 2016, **138**, 15011-15018.
11. L. Gao, Z. G. Zhang, L. Xue, J. Min, J. Zhang, Z. Wei and Y. Li, *Adv. Mater.*, 2016, **28**, 1884-1890.
12. L. Gao, Z. G. Zhang, H. Bin, L. Xue, Y. Yang, C. Wang, F. Liu, T. P. Russell and Y. Li, *Adv. Mater.*, 2016, **28**, 8288-8295.

13. H. Bin, L. Gao, Z. G. Zhang, Y. Yang, Y. Zhang, C. Zhang, S. Chen, L. Xue, C. Yang, M. Xiao and Y. Li, *Nat. Commun.*, 2016, **7**, 13651.
14. H. Bin, L. Zhong, Y. Yang, L. Gao, H. Huang, C. Sun, X. Li, L. Xue, Z. Zhang, Z. Zhang and Y. Li, *Adv. Energy Mater.*, 2017, **7**, 1700746.
15. L. Xue, Y. Yang, J. Xu, C. Zhang, H. Bin, Z. Zhang, B. Qiu, X. Li, C. Sun, L. Gao, J. Yao, X. Chen, Y. Yang, M. Xiao and Y. Li, *Adv. Mater.*, 2017, **29**, 1703344.
16. W. Liu, J. Zhang, Z. Zhou, D. Zhang, Y. Zhang, S. Xu and X. Zhu, *Adv. Mater.*, 2018, **30**, 1800403.
17. Y. Li, L. Zhong, B. Gautam, H. Bin, J. Lin, F. Wu, Z. Zhang, Z. Jiang, Z. Zhang, K. Gundogdu, Y. Li. and L. Liao, *Energy Environ. Sci.*, 2017, **10**, 1610.
18. B. Fan, W. Zhong, X. Jiang, Q. Yin, L. Ying, F. Huang and Y. Cao, *Adv. Energy Mater.*, 2017, **7**, 1602127.
19. R. Yu, S. Zhang, H. Yao, B. Guo, S. Li, H. Zhang, M. Zhang and J. Hou, *Adv. Mater.*, 2017, **29**, 1700437.
20. J. Wang, W. Wang, X. Wang, Y. Wu, Q. Zhang, C. Yan, W. Ma, W. You and X. Zhan, *Adv. Mater.*, 2017, **29**, 1702125.
21. T. Yan, H. Bin, Y. Yang, L. Xue, Z. Zhang and Y. Li, *Sci. China Chem.*, 2017, **60**, 537-544.
22. L. Ye, Y. Xiong, Q. Zhang, S. Li, C. Wang, Z. Jiang, J. Hou, W. You and H. Ade, *Adv. Mater.*, 2018, **30**, 1705485.
23. P. Cheng, J. Wang, Q. Zhang, W. Huang, J. Zhu, R. Wang, S. Y. Chang, P. Sun, L. Meng, H. Zhao, H. W. Cheng, T. Huang, Y. Liu, C. Wang, C. Zhu, W. You, X. Zhan and Y. Yang, *Adv. Mater.*, 2018, **30**, 1801501.
24. Y. Li, D. Qian, L. Zhong, J. Lin, Z. Jiang, Z. Zhang, Z. Zhang, Y. Li, L. Liao and F. Zhang, *Nano Energy*, 2016, **27**, 430-438.
25. Z. Luo, H. Bin, T. Liu, Z. G. Zhang, Y. Yang, C. Zhong, B. Qiu, G. Li, W. Gao, D. Xie, K. Wu, Y. Sun, F. Liu, Y. Li and C. Yang, *Adv. Mater.*, 2018, **30**, 1706124.
26. F. Zhao, S. Dai, Y. Wu, Q. Zhang, J. Wang, L. Jiang, Q. Ling, Z. Wei, W. Ma, W. You, C. Wang and X. Zhan, *Adv. Mater.*, 2017, **29**, 1700144.
27. Z. Li, S. Dai, J. Xin, L. Zhang, Y. Wu, J. Rech, F. Zhao, T. Li, K. Liu, Q. Liu, W. Ma, W. You, C. Wang and X. Zhan, *Mater. Chem. Front.*, 2018, **2**, 537-543.
28. S. C. Price, A. C. Stuart, L. Yang, H. Zhou and W. You, *J. Am. Chem. Soc.*, 2011, **133**, 4625-4631.
29. W. Li, L. Yan, H. Zhou and W. You, *Chem. Mater.*, 2015, **27**, 6470-6476.
30. J. Min, Z. Zhang, S. Zhang and Y. Li, *Chem. Mater.*, 2012, **24**, 3247-3254.
31. B. Liu, X. Chen, Y. He, Y. Li, X. Xu, L. Xiao, L. Li and Y. Zou, *J. Mater. Chem. A*, 2013, **1**, 570-577.
32. Z. Zhang, B. Peng, B. Liu, C. Pan, Y. Li, Y. He, K. Zhou and Y. Zou, *Polym. Chem.*, 2010, **1**, 1441-1447.
33. J. H. Kim, C. E. Song, N. Shin, H. Kang, S. Wood, I. N. Kang, B. J. Kim, B. Kim, J. S. Kim, W. S. Shin and D. H. Hwang, *ACS Appl. Mater. Interfaces*, 2013, **5**, 12820-12831.
34. L. Wang, H. Liu, S. Yang, C. Fu, Y. Li, Q. Li and Z. Huai, *ACS Appl. Mater. Interfaces*, 2018, **10**, 7271-7280.
35. L. Wang, H. Liu, Z. Huai and S. Yang, *ACS Appl. Mater. Interfaces*, 2017, **9**, 28828-28837.
36. S. Wood, J. Kim, D. Hwang and J. Kim, *Chem. Mater.*, 2015, **27**, 4196-4204.
37. D. Baran, A. Balan, S. Celebi, B. M. Esteban, H. Neugebauer, N. S. Sariciftci and L. Toppare, *Chem. Mater.*, 2010, **22**, 2978-2987.
38. L. Zhang, C. He, J. Chen, P. Yuan, L. Huang, C. Zhang, W. Cai, Z. Liu and Y. Cao, *Macromolecules*, 2010, **43**, 9771-9778.

39. H. Huang, H. Bin, Z. Peng, B. Qiu, C. Sun, L. Alex, Z. Zhang, C. Zhu, H. Ade, Z. Zhang and Y. Li, *Macromolecules*, 2018, **51**, 6028-6036.
40. X. Liu, C. Zhang, C. Duan, M. Li, Z. Hu, J. Wang, F. Liu, N. Li, C. J. Brabec, R. A. J. Janssen, G. C. Bazan, F. Huang and Y. Cao, *J. Am. Chem. Soc.*, 2018, **140**, 8934-8943.
41. H. Bin, Y. Yang, Z. Peng, L. Ye, J. Yao, L. Zhong, C. Sun, L. Gao, H. Huang, X. Li, B. Qiu, L. Xue, Z. Zhang, H. Ade and Y. Li, *Adv. Energy Mater.*, 2018, **8**, 1702324.
42. M. Chang, Y. Wang, Y. Yi, X. Ke, X. Wan, C. Li and Y. Chen, *J. Mater. Chem. A*, 2018, **6**, 8586-8594.
43. S. Chen, L. Zhang, C. Ma, D. Meng, J. Zhang, G. Zhang, Z. Li, P. C. Y. Chow, Z. W. W. Ma, K. S. Wong, H. Ade and H. Yan, *Adv. Energy Mater.*, 2018, **8**, 1702427.
44. Y. Gao, Z. Wang, J. Zhang, H. Zhang, K. Lu, F. Guo, Z. Wei, Y. Yang, L. Zhao and Y. Zhang, *Macromolecules*, 2018, **51**, 2498-2505.
45. Z. Zhang, S. Zhang, Z. Liu, Z. Zhang, Y. Li, C. Li and H. Chen, *Acta Phys. Chim. Sin.*, 2019, **35**, 394-400.
46. Y. Li, L. Zhong, F. Wu, Y. Yuan, H. Bin, Z. Jiang, Z. Zhang, Z. Zhang, Y. Li and L. Liao, *Energy Environ. Sci.*, 2016, **9**, 3429-3435.
47. A. Tang, B. Xiao, F. Chen, J. Zhang, Z. Wei and E. Zhou, *Adv. Energy Mater.*, 2018, **8**, 1801582.
48. X. Li, T. Yan, H. Bin, G. Han, L. Xue, F. Liu, Y. Yi, Z. Zhang, T. P. Russelle and Y. Li, *J. Mater. Chem. A*, 2017, **5**, 22588-22597.
49. C. Yan, W. Wang, T. Lau, K. Li, J. Wang, K. Liu, X. Lu and X. Zhan, *J. Mater. Chem. A*, 2018, **6**, 16638-16644.
50. Y. Gao, R. Zhu, Z. Wang, F. Guo, Z. Wei, Y. Yang, L. Zhao and Y. Zhang, *ACS Appl. Energy Mater.*, 2018, **1**, 1888-1892.
51. S. Shi, X. Chen, X. Liu, X. Wu, F. Liu, Z. G. Zhang, Y. Li, T. P. Russell and D. Wang, *ACS Appl. Mater. Interfaces*, 2017, **9**, 24451-24455.
52. S. Chen, Y. Liu, L. Zhang, P. C. Y. Chow, Z. Wang, G. Zhang, W. Ma and H. Yan, *J. Am. Chem. Soc.*, 2017, **139**, 6298-6301.
53. Q. Liu, Z. Xiao, T. Li, S. Yang, W. You, M. Wang and L. Ding, *Mater. Chem. Front.*, 2018, **2**, 1563-1567.
54. J. Zhu, Y. Wu, J. Rech, J. Wang, K. Liu, T. Li, Y. Lin, W. Ma, W. You and X. Zhan, *J. Mater. Chem. C*, 2018, **6**, 66-71.
55. Y. Lin, F. Zhao, S. K. K. Prasad, J. D. Chen, W. Cai, Q. Zhang, K. Chen, Y. Wu, W. Ma, F. Gao, J. X. Tang, C. Wang, W. You, J. M. Hodgkiss and X. Zhan, *Adv. Mater.*, 2018, **30**, 1706363.
56. J. D. Chen, Y. Q. Li, J. Zhu, Q. Zhang, R. P. Xu, C. Li, Y. X. Zhang, J. S. Huang, X. Zhan, W. You and J. X. Tang, *Adv. Mater.*, 2018, **30**, 1706083.
57. Y. Li, L. Zhong, J. Lin, F. Wu, H. Bin, Z. Zhang, L. Xu, Z. Jiang, Z. Zhang, F. Liu, T. P. Russell, Y. Li, L. Liao and S. R. Forrest, *Sol Rrl*, 2017, **1**, 1700107.
58. T. Li, H. Zhang, Z. Xiao, J. J. Rech, H. Niu, W. You and L. Ding, *Mater. Chem. Front.*, 2018, **2**, 700-703.
59. J. Zhu, Z. Ke, Q. Zhang, J. Wang, S. Dai, Y. Wu, Y. Xu, Y. Lin, W. Ma, W. You and X. Zhan, *Adv. Mater.*, 2018, **30**, 1704713.
60. Zh. Luo, G. Li, W. Gao, K. Wu, Z. Zhang, B. Qiu, H. Bin, L. Xue, F. Liu, Y. Li and C. Yang, *J. Mater. Chem. A*, 2018, **6**, 6874-6881.
61. P. Chao, L. Liu, J. Zhou, J. Qu, D. Mo, H. Meng, Z. Xie, F. He and Y. Ma, *ACS Appl. Energy Mater.*, 2018, **1**, 6549-6559.
62. S. Li, L. Ye, W. Zhao, S. Zhang, S. Mukherjee, H. Ade and J. Hou, *Adv. Mater.*, 2016, **28**, 9423-9429.
63. X. Xu, T. Yu, Z. Bi, W. Ma, Y. Li and Q. Peng, *Adv. Mater.*, 2018, **30**, 1703973.

64. J. Yuan, L. Qiu, Z. Zhang, Y. Li, Y. Chen and Y. Zou, *Nano Energy*, 2016, **30**, 312-320.
65. B. Guo, W. B. Li, G. P. Luo, X. Guo, H. F. Yao, M. J. Zhang, J. H. Hou, Y. F. Li and W. Y. Wong, *Acs Energy Lett.*, 2018, **3**, 2566.
66. H. Yao, Y. Chen, Y. Qin, R. Yu, Y. Cui, B. Yang, S. Li, K. Zhang and J. Hou, *Adv. Mater.*, 2016, **28**, 8283-8287.
67. W. Zhao, S. Li, H. Yao, S. Zhang, Y. Zhang, B. Yang and J. Hou, *J. Am. Chem. Soc.*, 2017, **139**, 7148-7151.
68. H. Bai, Y. Wang, P. Cheng, J. Wang, Y. Wu, J. Hou and X. Zhan, *J. Mater. Chem. A*, 2015, **3**, 1910-1914.
69. Y. Lin, Z. Zhang, H. Bai, J. Wang, Y. Yao, Y. Li, D. Zhu and X. Zhan, *Energy Environ. Sci.*, 2015, **8**, 610.
70. S. Li, L. Ye, W. Zhao, X. Liu, J. Zhu, H. Ade and J. Hou, *Adv. Mater.*, 2017, **29**, 1704051.
71. F. Liu, Z. Zhou, C. Zhang, T. Vergote, H. Fan, F. Liu and X. Zhu, *J. Am. Chem. Soc.*, 2016, **138**, 15523-15526.
72. S. Holliday, R. S. Ashraf, A. Wadsworth, D. Baran, S. A. Yousaf, C. B. Nielsen, C. H. Tan, S. D. Dimitrov, Z. Shang, N. Gasparini, M. Alamoudi, F. Laquai, C. J. Brabec, A. Salleo, J. R. Durrant and I. McCulloch, *Nat. Commun.*, 2016, **7**, 11585.
73. Y. Yi, H. Feng, M. Chang, H. Zhang, X. Wan, C. Li and Y. Chen, *J. Mater. Chem. A*, 2017, **5**, 17204.
74. W. Wang, C. Yan, T. K. Lau, J. Wang, K. Liu, Y. Fan, X. Lu and X. Zhan, *Adv. Mater.*, 2017, **29**, 1701308.
75. Y. Lin, Q. He, F. Zhao, L. Huo, J. Mai, X. Lu, C. J. Su, T. Li, J. Wang, J. Zhu, Y. Sun, C. Wang and X. Zhan, *J. Am. Chem. Soc.*, 2016, **138**, 2973-2976.
76. Y. Lin, J. Wang, Z. G. Zhang, H. Bai, Y. Li, D. Zhu and X. Zhan, *Adv. Mater.*, 2015, **27**, 1170-1174.
77. Z. Xiao, X. Jia, D. Li, S. Wang, X. Geng, F. Liu, J. Chen, S. Yang, T. P. Russell and L. Ding, *Sci. Bull.*, 2017, **62**, 1494-1496.
78. Y. Cui, C. Yang, H. Yao, J. Zhu, Y. Wang, G. Jia, F. Gao and J. Hou, *Adv. Mater.*, 2017, **29**, 1703080.
79. E. Wang, L. Hou, Z. Wang, S. Hellstrom, F. Zhang, O. Inganäs and M. R. Andersson, *Adv. Mater.*, 2010, **22**, 5240-5244.
80. Y. Liang, Z. Xu, J. Xia, S. T. Tsai, Y. Wu, G. Li, C. Ray and L. Yu, *Adv. Mater.*, 2010, **22**, 135-138.
81. Q. Peng, Q. Huang, X. Hou, P. Chang, J. Xu and S. Deng, *Chem. Commun.*, 2012, **48**, 11452-11454.
82. H. Hu, K. Jiang, G. Yang, J. Liu, Z. Li, H. Lin, Y. Liu, J. Zhao, J. Zhang, F. Huang, Y. Qu, W. Ma and H. Yan, *J. Am. Chem. Soc.*, 2015, **137**, 14149-14157.
83. L. Huo, T. Liu, X. Sun, Y. Cai, A. J. Heeger and Y. Sun, *Adv. Mater.*, 2015, **27**, 2938-2944.
84. D. Meng, D. Sun, C. Zhong, T. Liu, B. Fan, L. Huo, Y. Li, W. Jiang, H. Choi, T. Kim, J. Y. Kim, Y. Sun, Z. Wang and A. J. Heeger, *J. Am. Chem. Soc.*, 2016, **138**, 375-380.
85. H. Yao, L. Ye, J. Hou, B. Jang, G. Han, Y. Cui, G. M. Su, C. Wang, B. Gao, R. Yu, H. Zhang, Y. Yi, H. Y. Woo, H. Ade and J. Hou, *Adv. Mater.*, 2017, **29**, 1700254.
86. J. Wang, J. Zhang, Y. Xiao, T. Xiao, R. Zhu, C. Yan, Y. Fu, G. Lu, X. Lu, S. R. Marder and X. Zhan, *J. Am. Chem. Soc.*, 2018, **140**, 9140-9147.
87. T. Wang, T.-K. Lau, X. Lu, J. Yuan, L. Feng, L. Jiang, W. Deng, H. Peng, Y. Li and Y. Zou, *Macromolecules*, 2018, **51**, 2838-2846.
88. S. S. Li, L. Ye, W. C. Zhao, H. P. Yan, B. Yang, D. L. Liu, W. N. Li, H. Ade and J. H. Hou, *J. Am. Chem. Soc.*, 2018, **140**, 7159-7167.

89. L. Dou, C. Chen, K. Yoshimura, K. Ohya, W. Chang, J. Gao, Y. Liu, E. Richard and Y. Yang, *Macromolecules*, 2013, **46**, 3384-3390.
90. J. W. Jung, F. Liu, T. P. Russell and W. H. Jo, *Energy Environ. Sci.*, 2012, **5**, 6857-6961.
91. S. J. Xu, Z. Zhou, W. Liu, Z. Zhang, F. Liu, H. Yan and X. Zhu, *Adv. Mater.*, 2017, **29**, 1704510.
92. M. Li, Y. Liu, W. Ni, F. Liu, H. Feng, Y. Zhang, T. Liu, H. Zhang, X. Wan, B. Kan, Q. Zhang, T. P. Russell and Y. Chen, *J. Mater. Chem. A*, 2016, **4**, 10409.
93. H. Patil, A. Gupta, B. Alford, D. Ma, S. H. Privr, A. Bilic, P. Sonar and S. V. Bhosale, *Asian J. Org. Chem.*, 2015, **4**, 1096.
94. S. Li, L. Zhan, F. Liu, J. Ren, M. Shi, C. Z. Li, T. P. Russell and H. Chen, *Adv. Mater.*, 2018, **30**, 1705208.
95. J. Peet, J. Y. Kim, N. E. Coates, W. L. Ma, D. Moses, A. J. Heeger and G. C. Bazan, *Nat. Mater.*, 2007, **6**, 497-500.
96. Y. Zhong, M. T. Trinh, R. Chen, W. Wang, P. P. Khlyabich, B. Kumar, Q. Xu, C. Y. Nam, M. Y. Sfeir, C. Black, M. L. Steigerwald, Y. L. Loo, S. Xiao, F. Ng, X. Y. Zhu and C. Nuckolls, *J. Am. Chem. Soc.*, 2014, **136**, 15215-15221.
97. Y. Liu, G. Liu, R. Xie, Z. Wang, W. Zhong, Y. Li, F. Huang and Y. Cao, *Chem. Mater.*, 2018, **30**, 4331.
98. M. Wang, H. Wang, T. Yokoyama, X. Liu, Y. Huang, Y. Zhang, T. Q. Nguyen, S. Aramaki and G. C. Bazan, *J. Am. Chem. Soc.*, 2014, **136**, 12576-12579.
99. H. Feng, N. Qiu, X. Wang, Y. Wang, B. Kan, X. Wan, M. Zhang, A. Xia, C. Li, F. Liu, H. Zhang and Y. Chen, *Chem. Mater.*, 2017, **29**, 7908.
100. Y. Zhong, M. T. Trinh, R. Chen, G. E. Purdum, P. P. Khlyabich, M. Sezen, S. Oh, H. Zhu, B. Fowler, B. Zhang, W. Wang, C. Y. Nam, M. Y. Sfeir, C. T. Black, M. L. Steigerwald, Y. L. Loo, F. Ng, X. Y. Zhu and C. Nuckolls, *Nat. Commun.*, 2015, **6**, 8242.
101. H. Li, Y. J. Hwang, B. A. Courtright, F. N. Eberle, S. Subramaniyan and S. A. Jeneke, *Adv. Mater.*, 2015, **27**, 3266-3272.
102. Y. Liu, J. Zhao, Z. Li, C. Mu, W. Ma, H. Hu, K. Jiang, H. Lin, H. Ade and H. Yan, *Nat. Commun.*, 2014, **5**, 5293.
103. D. Xie, T. Liu, W. Gao, C. Zhong, L. Huo, Z. Luo, K. Wu, W. Xiong, F. Liu, Y. Sun and C. Yang, *Sol Rrl*, 2017, **1**, 1700074.
104. K. Kawashima, Y. Tamai, H. Ohkita, I. Osaka and K. Takimiya, *Nat. Commun.*, 2015, **6**, 10085.
105. V. Vohra, K. Kawashima, T. Kakara, T. Koganezawa, I. Osaka, K. Takimiya and H. Murata, *Nat. Photonics*, 2015, **9**, 403.
106. H. Yao, Y. Cui, R. Yu, B. Gao, H. Zhang and J. Hou, *Angew. Chem. Int. Ed.*, 2017, **56**, 3045-3049.
107. E. Zhou, J. Cong, K. Hashimoto and K. Tajima, *Energy Environ. Sci.*, 2012, **5**, 9756.
108. K. H. Hendriks, W. Li, M. M. Wienk and R. A. Janssen, *J. Am. Chem. Soc.*, 2014, **136**, 12130-12136.
109. W. Li, K. H. Hendriks, A. Furlan, M. M. Wienk and R. A. Janssen, *J. Am. Chem. Soc.*, 2015, **137**, 2231-2234.
110. S. Li, L. Ye, W. Zhao, S. Zhang, H. Ade and J. Hou, *Adv. Energy Mater.*, 2017, **7**, 1700783.
111. A. Mishra, M. L. Keshtov, A. Looser, R. Singhal, M. Stolte, F. Wurthner, P. Buerle and G. D. Sharma, *J. Mater. Chem. A*, 2017, **5**, 14887.
112. K. Chen, J. Salinas, H. Yip, L. Huo, J. Hou and A. K.-Y. Jen, *Energy Environ. Sci.*, 2012, **5**, 9551-9557.

113. R. Betancur, P. Romero-Gomez, A. Martinez-Otero, X. Elias, M. Maymo' and J. Martorell, *Nat. Photonics*, 2013, **7**, 995-1000.
114. G. Xu, L. Shen, C. Cui, S. Wen, R. Xue, W. Chen, H. Chen, J. Zhang, H. Li, Y. Li and Y. Li, *Adv. Funct. Mater.*, 2017, **27**, 1605908.
115. H. Shi, R. Xia, C. Sun, J. Xiao, Z. Wu, F. Huang, H. Yip and Y. Cao, *Adv. Energy Mater.*, 2017, **7**, 1701121.
116. W. J. Silva, H. P. Kim, A. R. M. Yusoffb and J. Jang, *Nanoscale*, 2013, **5**, 9324-9329.
117. Y. Wang, B. Jia, F. Qin, Y. Wu, W. Meng, S. Dai, Y. Zhou and X. Zhan, *Polym.*, 2016, **107**, 108-112.
118. M. B. Upama, M. Wright, N. K. Elumalai, M. A. Mahmud, D. Wang, C. Xu and A. Uddin, *ACS Photonics*, 2017, **4**, 2327-2334.
119. T. Li, S. Dai, Z. Ke, L. Yang, J. Wang, C. Yan, W. Ma and X. Zhan, *Adv. Mater.*, 2018, **30**, 1705969.
120. B. Jia, S. Dai, Z. Ke, C. Yan, W. Ma and X. Zhan, *Chem. Mater.*, 2018, **30**, 239-245.
121. Y. Li, J. Lin, X. Che, Y. Qu, F. Liu, L. Liao and S. R. Forrest, *J. Am. Chem. Soc.*, 2017, **139**, 17114-17119.
122. F. Liu, Z. Zhou, C. Zhang, J. Zhang, Q. Hu, T. Vergote, F. Liu, T. P. Russell and X. Zhu, *Adv. Mater.*, 2017, **29**, 1606574.
123. C. Chang, L. Zuo, H. Yip, Y. Li, C. Li, C. Hsu, Y. Cheng, H. Chen and A. K.-Y. Jen, *Adv. Funct. Mater.*, 2013, **23**, 5084-5090.
124. L. Dou, W. Chang, J. Gao, C. Chen, J. You and Y. Yang, *Adv. Mater.*, 2013, **25**, 825-831.
125. Z. Liu, P. You, S. Liu and F. Yan, *ACS Nano.*, 2015, **9**, 2026–12034.
126. C. C. S. Chien, H. Yip, J. F. Salinas, C. Li , K. Chen, F. Chen, W. Chen and A. K.-Y. Jen, *Adv. Energy Mater.*, 2013, **3**, 417-423.
127. Z. M. Bailey, M. G. Christoforo, P. Gratia, A. R. Bowring, P. Eberspacher, G. Y. Margulis, C. Cabanetos, P. M. Beaujuge, A. Salleo and M. D. McGehee, *Adv. Mater.*, 2013, **25**, 7020-7026.